



AMAP CORE – ATMOSPHERIC PART

from 1990 to 2015

Technical Report from DCE – Danish Centre for Environment and Energy

No. 101

2017



AARHUS
UNIVERSITY

DCE – DANISH CENTRE FOR ENVIRONMENT AND ENERGY

AMAP CORE – ATMOSPHERIC PART

from 1990 to 2015

Technical Report from DCE – Danish Centre for Environment and Energy

No. 101

2017

Henrik Skov
Andreas H. Massling
Ingeborg E. Nielsen
Claus Nordstrøm
Rossana Bossi
Katrin Vorkamp
Jesper Christensen
Martin Mørk Larsen
Kaj Mantzius Hansen
Jesper Baltzer Liisberg
Maria Bech Poulsen

Aarhus University, Department of Environmental Science



AARHUS
UNIVERSITY

DCE – DANISH CENTRE FOR ENVIRONMENT AND ENERGY

Data sheet

Series title and no.:	Technical Report from DCE – Danish Centre for Environment and Energy No. 101
Title:	AMAP CORE - ATMOSPHERIC PART
Authors:	Henrik Skov, Andreas H. Massling, Ingeborg E. Nielsen, Claus Nordstrøm, Rossana Bossi, Katrin Vorkamp, Jesper Christensen, Martin Mørk Larsen, Kaj Mantzius Hansen, Jesper Baltzer Liisberg and Maria Bech Poulsen
Institution:	Institut for Miljøvidenskab (ENVS), Aarhus Universitet
Publisher:	Aarhus University, DCE – Danish Centre for Environment and Energy ©
URL:	http://dce.au.dk/en
Year of publication:	September 2017
Editing completed:	July 2017
Referee:	Ole Hertel
Quality assurance, DCE:	Vibeke Vestergaard
Financial support:	DANCEA via the Danish Environmental Protection Agency
Please cite as:	Henrik Skov, Andreas H. Massling, Ingeborg E. Nielsen, Claus Nordstrøm, Rossana Bossi, Katrin Vorkamp, Jesper Christensen, Martin Mørk Larsen, Kaj Mantzius Hansen, Jesper Baltzer Liisberg and Maria Bech Poulsen. 2017. AMAP CORE - ATMOSPHERIC PART. Results from Villum Research Station. Aarhus University, DCE – Danish Centre for Environment and Energy, 77 pp. Technical Report from DCE – Danish Centre for Environment and Energy No. 101 http://dce2.au.dk/pub/TR101.pdf
	Reproduction permitted provided the source is explicitly acknowledged
Abstract:	This report describes the results obtained in the Danish contribution to the atmospheric part of the Arctic Monitoring and Assessment Program (AMAP). Results of measurements carried out at Villum Research Station, Station Nord from 1990 to 2015 are reported. A series of particle bound compounds and gasses relevant for determining the antropogenic impact on the sensitive Arctic environment have been measured. The results have been used to make new parameterisation of the Danish Eulerian model as well as to constrain the model. The results are reported to AMAP, EMEP and to WMO-Global Atmospheric Watch. The data have been analysed for statistical significant trends and the connection between emissions and observed concentrations was investigated using a combination of models and measurements.
Keywords:	Arctic, atmosphere, pollutants, AMAP, measurements, modelling
Layout:	Majbritt Pedersen-Ulrich
Front page photo:	Henrik Skov
ISBN:	978-87-7156-277-4
ISSN (electronic):	2245-019X
Number of pages:	77
Internet version:	The report is available in electronic format (pdf) at http://dce2.au.dk/pub/TR101.pdf

Contents

1	Introduction	5
2	Site description	7
3	Experimental Section	9
3.1	Filter pack sampler	11
3.2	High Volume Sampler	14
3.3	Monitors (GEM, CO, O ₃)	15
3.4	Surface snow samples	17
3.5	DEHM model	18
4	Results and Discussion	20
4.1	Filter pack sampler results	20
4.2	Modelling 37 years of Sulphate and Sulphur dioxide	35
4.3	Results from High Volume Sampler	38
4.4	Monitors (GEM and O ₃)	49
4.5	PFAS in snow	52
4.6	Mercury in snow	53
5	Conclusion and recommendations	55
5.1	SO _x	55
5.2	Other inorganic species	56
5.3	Persistent Organic Pollutants	56
5.4	Mercury and ozone	56
5.5	Snow samples	57
6	Acknowledgement	58
7	References	59
8	Appendix A	65
8.1	MATERIALS AND METHODS	65
8.2	Analytical method neutral PFAS	68
9	Appendix B	71
9.1	List of publication connected to AMAP	71
10	Appendix C	75
10.1	Abbreviations and wordlist	75

1 Introduction

This report describes the results obtained in the Danish contribution to the Arctic Monitoring and Assessment Program (AMAP), the atmospheric part.

In addition, AMAP data is also reported to the European Monitoring and Evaluation Programme (EMEP) and the World Meteorological Organisation-Global Atmospheric Watch Programme (WMO-GAW). The data also forms the basis for a long series of scientific collaborations through joint campaigns and studies. These activities typically focus on key processes and thus provide us with fundamental knowledge that makes it easier to understand observed trends and dynamics. A reference list of all peer reviewed articles is found in Appendix B.

Our activities started in a small hut in 1990 at Station Nord in North Greenland and from the beginning; we have received funding from the Danish Environmental Protection Agency with means from the MIKA/DANCEA funds for Environmental Support to the Arctic Region to carry out monitoring of contaminants that are transported into the Arctic. The work is part of the Danish contribution to the Circum-Polar monitoring program AMAP.

Since 1990 a selection of atmospheric pollutants has been measured at Station Nord with a break between 2002 and 2007, where the activities were moved to Nuuk on the west coast of Greenland. Station Nord is located in the uppermost northeastern corner of Greenland, see Figure 1.1. From 1990 to 1997 measurements were performed at Long Wave Hut located at the end of the runway. In 1995 measurements were moved to a newly built hut, Flygers Hut, located 2.5 km outside the complex of Station Nord buildings, see Figure 2.1, resulting in three years with double observations.

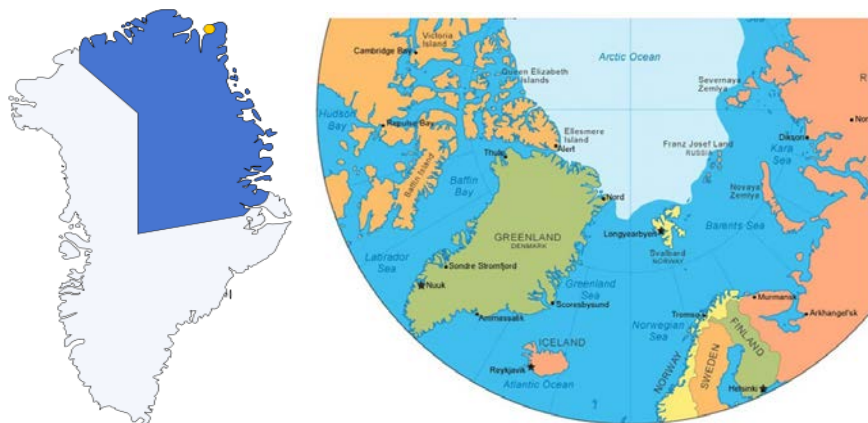


Figure 1.1. Left: Greenland with indication of the largest Natural Reserve in the world (blue) and the position of Station Nord (yellow dot), where VRS is located. Right: The Northern Hemisphere with Station Nord (Nord) marked.

In 2013, Department of Environmental Science, Aarhus University received a grant from the Villum Foundation on 70.5 mil kr. for construction of a new research infrastructure at Station Nord, the Villum Research Station, Station

Nord (VRS). The inauguration of the Station was held on 8th July 2015. The reason for the grant is the accelerating temperature increase caused by anthropogenic emissions of especially CO₂(1). The temperature rise in the Arctic has increased twice as fast as the average for the rest of the world (1) and with large difference within the Arctic. In the Fram Strait east of VRS, 8-10 °C temperature increase has been estimated by the end of this century (2). VRS has an ideal position for studying causes and consequences of the changing climate, as it is basically located in the “bull’s eye”. Furthermore, large seasonal variations of pollutants and chemistry are observed at VRS (3-11). Therefore studies will provide knowledge not only about Arctic changes, but observations will also be an indicator for global changes. VRS is thus attractive for the international scientific community and the research facilities have already been used by scientists from all over the world. Due to the open data philosophy, these new activities also strengthen the AMAP results.

In recent years, changes in source strength and source positions have been the main driver for observations of pollutants at VRS. The world society is also under rapid change and the interest in the Arctic is increasing mainly due to possible new shipping routes and in the search for new resources such as oil and minerals.

In the present report, we present long time series of atmospheric concentrations of aerosols and selected gasses. Focus is on recent years, but the results are always evaluated in a broader time perspective. Analysis of possible causes for observed trends and of the processes behind are presented.

2 Site description

Station Nord is a Danish military station. An important part of the station is the runway, since the only access to the station is by plane. The station serves as emergency landing strip and as service for the Sirius Patrol that maintain the Danish Kingdom's sovereignty of North Greenland. The station is run by the Danish military, but it serves moreover as a step stone for researchers that want to conduct research in North Greenland e.g. Peary Land. Besides the runway, the station consists of a series of houses for accommodation, workshops etc. for supporting the military activities. A close collaboration between Danish military and Aarhus University is established and VRS uses the Station Nord canteen, this means that researchers and soldiers are eating together and discussing the events of the day.

VRS consists of three parts, the Base Station, the Mobile Station and the Air Station (www.villumresearchstation.dk):

The Base Station located at Station Nord consists of three buildings with living quarters, laboratories and storage rooms; see Figure 2.1 and 2.2. It will provide a platform for joint studies of air pollution, climate, geology, and biological processes in ecosystems in the neighbourhood of Station Nord. The Base Station has accommodation for 14 scientists at a time.

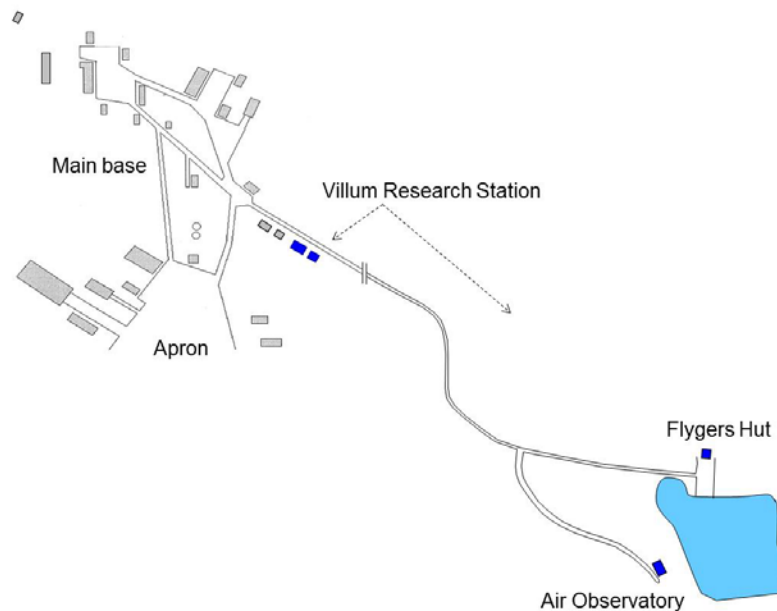


Figure 2.1. Map of the position of Flyers Hut and the buildings of Villum Research Station.

A detailed description of the military station, Station Nord, and its possible impact on the nearby surroundings is found elsewhere (6).



Figure 2.2. Villum Research Station. Photo: Bjarne Jensen

The Mobile Station includes mobile laboratories and living quarters consisting of tents and vehicles. The Mobile Station makes it possible to do atmospheric, terrestrial, sea-ice and marine research at long distances away from Station Nord.

The Air Station consist of drones and ground based remote sensors that makes it possible to study vertical profiles of the atmosphere to an altitude of a few kilometres, and to make aerial observations of snow, sea-ice and the terrestrial landscape by remote sensing.

VRS is the second most northern, permanently open station in the Arctic only exceeded by Alert, Canada. It has all of the logistic requirements and possibilities, which are necessary for being a major international platform for scientific studies focused on the Arctic cryosphere, nature and interaction with humans. It is located in the farthest north eastern corner of Greenland on the north - south oriented peninsula Prinsesse Ingeborgs Halvø (81°36' N 16°40' W) which northern end is a 20 x 15 km² Arctic lowland plain. It is an important logistic site for many scientific research activities in the Greenlandic National Park, in North Greenland and provides a different type of data set than any other Arctic stations; see Table 3.1 to Table 3.3 and www.villumresearchstation.dk.

3 Experimental Section

This report presents results obtained as part of the Danish contribution to AMAP. A long series of compounds and parameters are measured in the atmosphere at Villum Research Station, Station Nord in North Greenland. A complete list of all compounds, parameters and instruments at VRS is found at www.villumresearchstation.dk and a substantial part is summarised in Appendix C.

Table 3.1, Table 3.2, and Table 3.3 show the compounds and parameters reported here.

Table 3.1. List of parameters of compounds and parameters.

Activities	Data availability	Instruments
Filter pack measurements of SO ₂ , SO ₄ ²⁻ , NO ₃ ⁻ and NH ₄ ⁺	1990 - June 2002 and July 2006 - present	IC and segmented flow analyzer
Filter pack measurements of elements from Al and higher (except Cl, and Hg)	1990 - June 2002 and July 2006- present	ICP-MS
O ₃	1997-2002 and 2006 – present	O ₃ monitor using UV absorption
Gaseous Elemental Mercury (GEM)	August 1999 – 2002 and 2006- present	GEM monitor using Cold vapour fluorescence spectroscopy
Black Carbon	2008 - present	(PSAP, MAAP)
CO	July 2016 - present	CO monitor using IR absorption spectroscopy. From 2012 a CO monitor using gas chromatography and a Hg reduction detector
High volume sampling equipped with particle filter and PUF, XAD, PUF sandwich plug to measure chlorinated pesticides.	July 2006 - present	GC-HRMS, LC-MS-MS
Brominated flame retardants measured with high volume sampler (same as chlorinated pesticides)	July 2006 - present	
Persistent fluorinated compounds measured with a specially designed high volume sampler	January 2007 - present	
CH ₄ and CO ₂ gradients with a Picaro; Leico	January 2012 - present	Cavity ring down method
Meteorological parameters*	At least from 1961	Synoptic data
Climate: Wind speed, wind direction, temperature, relative humidity, solar flux (in and out), precipitation, snow depth,	July 2014 - present	Set up by ASIAQ (Greenland)

A. Chlorinated compounds:**Table 3.2.** Persistent organic compounds measured with a High Volume sampler sucking 500 L min⁻¹ through a filter and a PUF-XAD-PUF cartridge.

Matrix	Acronym	Full name	Measured in biota
Air	HCB	Hexachlorobenzen	Yes
Air	α-HCH	α-hexachlorocyclohexane	Yes
Air	β-HCH	β-hexachlorocyclohexane	Yes
Air	γ-HCH (Lindane)	γ-hexachlorocyclohexane	Yes
Air	δ-HCH	δ-hexachlorocyclohexane	No
Air	Heptachlor	Heptachlor	No
Air	Heptachlor epoxide	Heptachlor epoxide	No
Air	Aldrin	Aldrin	No
Air	Dieldrin	Dieldrin	No
Air	Endrin	Endrin	No
Air	trans-Chlordane	trans-Chlordane	Yes
Air	cis-Chlordane	cis-Chlordane	Yes
Air	o,p'-DDT	o,p'-DDT	Yes
Air	p,p'-DDT	p,p'-DDT	Yes
Air	o,p'-DDE	o,p'-DDE	Yes
Air	p,p'-DDE	p,p'-DDE	Yes
Air	o,p'-DDD	o,p'-DDD	No
Air	p,p'-DDD	p,p'-DDD	Yes
Air	α-Endosulfan	α-Endosulfan	Yes*
Air	β-Endosulfan	β-Endosulfan	Yes*
Air	Endosulfan sulphate	Endosulfan sulphate	Yes*
Air	trans-Nonachlor	trans-Nonachlor	Yes
Air	cis-Nonachlor	cis-Nonachlor	Yes
Air	Endrin ketone	Endrin ketone	No
Air	Metoxychlor	Metoxychlor	No

*It is not part of the monitoring program but has been measured campaign wise (New Contaminant project).

B. Brominated compounds:

Matrix	Acronym	Full name	Measured in biota
Air	BDE 17	Polybrominated diphenylether 17	Yes
Air	BDE 28	Polybrominated diphenylether 28	Yes
Air	BDE 47	Polybrominated diphenylether 47	Yes
Air	BDE 66	Polybrominated diphenylether 66	Yes
Air	BDE 71	Polybrominated diphenylether 71	No
Air	BDE 85	Polybrominated diphenylether 85	Yes
Air	BDE 99	Polybrominated diphenylether 99	Yes
Air	BDE 100	Polybrominated diphenylether 100	Yes
Air	BDE 138	Polybrominated diphenylether 138	No
Air	BDE 153	Polybrominated diphenylether 153	Yes
Air	BDE 154	Polybrominated diphenylether 154	Yes
Air	BDE 183	Polybrominated diphenylether 183	Yes
Air	BDE 180	Polybrominated diphenylether 180	No
Air	BDE 209	Polybrominated diphenylether 209	Yes
Air	α-HBCD	α-Hexabromcyclododecane	Yes
Air	β-HBCD	β-Hexabromcyclododecane	Yes
Air	γ-HBCD	γ-Hexabromcyclododecane	Yes

*Other CAS-numbers for HBCD: 25637-99-4 or 3194-55-6; we do not have this number

C. Perfluoroalkyl substances (PFAS):

Matrix	Acronym	Full name	Measured in biota
Air	4:2 FTOH	4:2-fluorotelomer alcohol	No
Air	6:2 FTOH	6:2-fluorotelomer alcohol	No
Air	8:2 FTOH	8:2-fluorotelomer alcohol	No
Air	10:2 FTOH	10:2-fluorotelomer alcohol	No
Air	N-Me-FOSA	N-methyl-perfluorooctanesulfonamide	No
Air	N-Et-FOSA	N-ethyl-perfluorooctanesulfonamide	No
Air	N-Me-FOSE	N-methyl-perfluorooctanesulfonamidoethanol	No
Air	N-Et-FOSE	N-ethyl-perfluorooctanesulfonamidoethanol	No
Snow	PFBS	Perfluorobutane sulfonate	Yes
Snow	PFHxS	Perfluorohexane sulfonate	Yes
Snow	PFHpS	Perfluoroheptane sulfonate	Yes
Snow	PFOS	Perfluorooctane sulfonate	Yes
Snow	PFDS	Perfluorodecane sulfonate	Yes
Snow	PFOSA	Perfluorooctane sulfonamide	Yes
Snow	PFHxA	Perfluorohexanoic acid	Yes
Snow	PFHpA	Perfluoroheptanoic acid	Yes
Snow	PFOA	Perfluorooctanoic acid	Yes
Snow	PFNA	Perfluorononanoic acid	Yes
Snow	PFDA	Perfluorodecanoic acid	Yes
Snow	PFUnA	Perfluoroundecanoic acid	Yes
Snow	PFDoA	Perfluorododecanoic acid	Yes
Snow	PFTTrA	Perfluorotridecanoic acid	Yes
Snow	PFTeA	Perfluorotetradecanoic acid	Yes

Table 3.3. Meteorological parameters measured at VRS.

Activities	Data availability	Instruments
Temperature	August 2014	
Relative humidity	August 2014	
Wind direction	August 2014	
Wind speed	August 2014	
Precipitation	August 2014	
Radiation balance	August 2014	
Snow depth	August 2014	
Boundary layer height	August 2014	Ceilmeter
Vertical wind profile	Spring 2016	Wind LIDAR

3.1 Filter pack sampler

In 1990 a filter pack sampler was installed at Station Nord. The purpose of this filter pack sampler was to collect particulate mass and inorganic gases on a monitoring base. The particle filters were analysed for sulphate- (SO_4^{2-}), ammonium- (NH_4^+) and nitrate (NO_3^-) ions, and several heavy metals. From 1990 to 1997, the filter pack sampler was located at the "LW hut", which is a housing located at the end of the runway of the military camp. In 1995, measurements were moved to "Flygers hut" about 2.5 km south of the centre of the military camp. The boom with the filter holders was installed about 4.5 metres above the ground at the "LW hut" and "Flygers hut". In 2002, the location of

the filter pack sampler was moved from North Greenland to Nuuk in South-east Greenland, but moved back again in 2007 to "Flygers Hut".

During normal operation 7 filters, each consisting of three consecutive filters are plugged into the filter holders. The first filter collects particles whereas the second and third filter is impregnated with special adsorbing chemicals for collection of selected gases. The three units are subject to different extractions and analyses listed in Table 3.4.

The flow through the filters is 40 L min^{-1} . The flow is adjusted towards a traceable standard on regular intervals as it is used to calculate the mass concentrations of the analysed species. In addition, the flow control unit is operating eight valves of the same type to switch the sampling from filter unit 1 to filter unit 7 at predefined time steps. The filter pack sampler has been operated since 1990 with the same time schedule collecting aerosol particles and gases on the filter units for one week starting Monday, 24:00, local time and ending one week later on Monday, 24:00, local time. In this way about 52 to 53 weekly samples are produced during a full calendar year.

Table 3.4. List of analytical methods used for different species analysed at Villum Research Station (VRS) at Station Nord (SN) in North Greenland.

Component	Phase	Analytical technique
Al	Particle	PIXE, ICP-MS
As	Particle	PIXE, ICP-MS
Ba	Particle	PIXE, ICP-MS
Br	Particle	PIXE, ICP-MS, Dual-IC
Ca	Particle	PIXE, ICP-MS, Dual-IC
Cu	Particle	PIXE, ICP-MS
Cl	Particle	PIXE, ICP-MS, IC
Co	Particle	PIXE, ICP-MS
Cr	Particle	PIXE, ICP-MS
Cu	Particle	PIXE, ICP-MS
Fe	Particle	PIXE, ICP-MS
Ga	Particle	PIXE, ICP-MS
K	Particle	PIXE, ICP-MS, Dual-IC
Mg	Particle	PIXE, ICP-MS, Dual-IC
Mn	Particle	PIXE, ICP-MS
Mo	Particle	PIXE, ICP-MS
Na	Particle	PIXE, ICP-MS, Atomic absorption, Cationchromatography, Dual-IC
Ni	Particle	PIXE, ICP-MS
Pb	Particle	PIXE, ICP-MS
Rb	Particle	PIXE, ICP-MS
S	Particle	PIXE, ICP-MS
Sb	Particle	PIXE, ICP-MS
Se	Particle	PIXE, ICP-MS
Si	Particle	PIXE, ICP-MS
Sr	Particle	PIXE, ICP-MS
Ti	Particle	PIXE, ICP-MS
V	Particle	PIXE, ICP-MS
Zn	Particle	PIXE, ICP-MS
HNO ₃	Gas	Auto analyzer, IC
NO ₃ ⁻	Particle	Auto analyzer, IC
SO ₂	Gas	IC
SO ₄ ²⁻	Particle	IC
NH ₃	Gas	Auto analyzer,
NH ₄ ⁺	Particle	Auto analyzer,

Table 3.4 illustrates that, the analytical technique has changed for some of the compounds during the years. The reason is that techniques have developed over the years, and it was the intention to choose the best methods, with optimal detection limit, to carry out the analysis at the lowest possible cost. As general information, it can be stated that proton induced X-ray emission (PIXE) was used in the time period between 1990 – 2010 for analysis of alumina and elements with higher mass (except mercury). The PIXE was constructed as a custom-built setup, and this technique was replaced by ICP-MS in 2010.

In Chapter 4, time series, yearly trends and seasonal variations of selected species are presented and discussed. Focus is on the distribution between natural and anthropogenic sources and on source regions related to the observed levels at VRS. The long-range transport of pollutants from mid-latitudes and other areas of the world with high anthropogenic activity to the high Arctic is of major concern. This transport and deposition can have substantial impact on the Arctic ecosystems changing fauna and flora and thus affect the complete biological and natural cycle in this sensitive area.

3.2 High Volume Sampler

Weekly air samples of about 5000 m³ were collected using a High-Volume Sampler (HVS) from (Digitel, Hegnau, Switzerland) operating at a flow rate of 0.5 m³ min⁻¹. The sampler is placed in a hut at the centre of Station Nord. The position is not ideal, but was chosen due to lack of power at Flygers Hut. In the end of the measurement period reported here, it was moved to the new Air Observatory.

The HVS is equipped with a heated sampling head (outside) for sampling total suspended particles. Via a stainless steel tube, sampled air is thereafter sucked through a PM₁₀ head that is located inside the hut before finally reaching a particle filter and a cartridge. The impactor surface in the PM₁₀ head is coated with silicone grease, to avoid bounce-off of larger particles. The grease is replaced 4 times a year during maintenance visits. A 15 cm d. quartz fibre filter is used for particle collection, and a cartridge sandwich of polyurethane foam/XAD-2/polyurethane foam is used for vapour phase collection. The polyurethane foam and XAD-2 are cleaned before use with Soxhlet extraction for 8 hours using dichloromethane as solvent. Quartz filters are baked at 450 °C for 24 hours. After sampling, cartridges and filters are kept at -20 °C. For analysis of the different classes of compounds one sample from each month is extracted and analysed. The analysis program is the following: one sample analysed for organochlorine pesticides (OCPs) and polybrominated phenyl ethers (PBDEs), one sample analysed for neutral perfluoroalkylated substances (PFASs) and one sample analysed for hexabromocyclododecane (HBCDD). HBCDD, a brominated flame retardant, has been included in the analysis of organic chemicals at VRS since 2012, while results for the other POPs are available since 2008. As HBCDD is attached only to particles in the atmosphere (12), only filters were analysed. The main use of HBCDD has been in polystyrene foams, for example in building insulations. In contrast to polybrominated diphenyl ethers (PBDEs), HBCDD has mainly been used in Europe (13). The technical product consists of several isomers, with γ -, α - and β -HBCDD accounting for 75-89%, 10-13% and 1-12% of HBCDD, respectively (14). The chemical structure of HBCDD is given in Figure 3.1. HBCDD is considered as a substance of very high concern by the European Chemicals Agency and a priority hazardous substance under the European Union Water Framework Directive (15, 16). It is on OSPAR's List of Chemicals for Priority Action (17) and a persistent organic pollutant (POP) in the context of the POP protocol of the UNECE Convention on Long-Range Transboundary Air Pollution (18). Since 2013, HBCDD has been included in the Stockholm Convention; however, the convention allows time-limited exemptions of HBCDD use in expanded and extruded polystyrene in buildings (19).

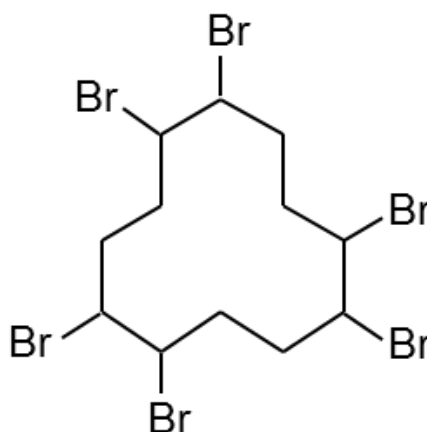


Figure 3.1. Chemical structure of hexabromocyclododecane (HBCDD).

The last sample collected during a month is kept in the freezer for special analyses. A list of the analysed compounds is presented in Table 3.2 and 3.3 and is also seen in Appendix C.

The samples analysed for OCPs and PBDEs are spiked with ^{13}C -labelled isotopes before extraction, extracted with n-hexane/acetone (4:1, v/v), and cleaned on silica columns. Identification and quantification of the target compounds were performed with gas chromatography - high resolution mass spectrometry (GC-HRMS).

Samples analysed for neutral PFASs are spiked with deuterium-labelled isotopes, extracted with MTBE/acetone (1/1, v/v) and analysed by GC-MS with positive chemical ionization (PCI).

For the chemical analysis, the filters were spiked with ^{13}C -labelled standards of each isomer and extracted using hexane:acetone (4:1). After clean-up and volume reduction, the samples were analysed by high performance liquid chromatography (HPLC) with tandem mass spectrometry (MS-MS).

A detailed description of the analytical methods is available in Appendix A.

Quality assurance/quality control procedure were the following: three laboratory blanks and three field blanks were extracted for each sampling year, thereafter concentrations of target analytes in samples were corrected for recovery of correspondent or similar labelled surrogate standards and finally concentrations were corrected for field blank values.

3.3 Monitors (GEM, CO, O₃)

Ozone has been measured since 1996. Though different instruments have been applied we estimate that the uncertainty is unchanged in the measurements. The basic principle in all instruments is absorption of UV light at 254 nm. The stability of the instrument is ensured by addition of known concen-

trations of ozone from an internal ozone generator. The uncertainty is assessed on 95 % confidence level to be <7% for concentrations above 20 ppbv and 1.4 ppbv for concentrations below 20 ppbv.

Since 1999, GEM has been measured by a TEKRAN 2537 mercury analyser. In the first years, funding was only available for 6 month per year and thus the data coverage over the entire year is limited to spring and summer. Several generations of the instrument has been used (A, B and X versions), but we estimate also in this case that the uncertainty of measuring GEM is unchanged during the years. The principle of the instrument is as follows: a measured volume of sample air is drawn through a gold trap that quantitatively retains elemental mercury. The collected mercury is desorbed from the gold trap by heat and is transferred by argon into the detection chamber, where the amount of mercury is detected by cold vapour atomic fluorescence spectroscopy. The detection limit is 0.1 ng m⁻³ and the reproducibility for concentrations above 0.5 ng m⁻³ is within 20 % (at a 95 % confidence interval) based on parallel measurements with two TEKRAN 2537A mercury analysers. The calibration of the instrument is checked every 25 hours by adding known quantities of elemental mercury to the detection system from an internal permeation source that is traceable to a primary standard.

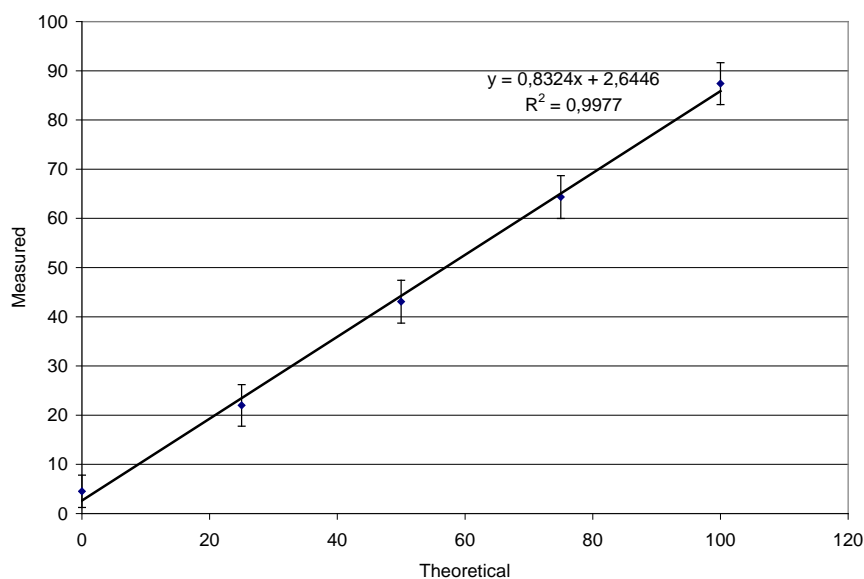


Figure 3.2. Calibration curve; measured concentrations of CO against known concentrations (theoretical). Unit; ppbv.

CO was first measured by GC followed by a mercury oxide reduction detector, where mercury oxide is reduced to elemental mercury and detected by UV absorption. Unfortunately the data appeared to be unreliable and the instrument was changed to a TELEDYNE API T300 U differential infrared absorption spectroscopy. The detection limit is 10 ppbv (3 times standard deviation on blanks) and with an uncertainty of 15 % on a 95 % confidence interval. The calibration curve is shown in Figure 3.2 and the instrument has been thoroughly checked and is ready for installation at the Station. We anticipated having measurements with the TELEDYNE instrument already in January

2016, but the process was delayed due to troubles with the belonging calibration unit, which has to be returned to the manufactory for repair.

The instrument will thus first be installed in February 2017 and thus there is not any further CO data to be shown.

3.4 Surface snow samples

In the later years there have been collected snow samples for analyses for selected POPs and for Hg.

3.4.1 PFAS

Surface snow samples are collected from October to May every second month. Samples of snow are collected with a metal shovel and placed in a plastic bag. The snow is slowly melted and transferred from the bag into 5 litre plastic bottles. The samples are then shipped to Denmark, where they are analysed.

Two litre samples are analysed in duplicate for acidic PFAS (perfluorinated alkyl substances). The samples are spiked with ¹³C-labelled isotopes and extracted with solid phase extraction (SPE). The extracts are analysed with liquid chromatography-tandem mass spectrometry (LC-MS-MS). The details of the analytical method are described in Bossi et al. (2015). The compounds included in the analyses are summarised in Table 3.2.

3.4.2 Mercury

Wet deposition of mercury was also investigated in collaboration with National Resources Canada (NRCAN) from Canada. They have developed a new wet-only sampler to be used in Arctic (20). They tested the sampler at several Arctic stations in Canada, however, deploying it to Station Nord, the wet only failed to work and is currently at Department of Environmental Science (ENVS) for modifications.

Therefore a series of snow samples are collected for the analysis of mercury in surface snow. Sample bottles were washed with 10 % nitric acid and were controlled by adding deionised water and analysing the blanks prior to sending them to VRS. 5 ml of 10 % nitric acid was added to the sampling bottles to fixate mercury.

Samples are collected at long distances from the central area of Station Nord (and VRS) in pristine snow. The sample flask is un-screwed while keeping the opening away from the breathing zone. The samples are collected wearing gloves and by pushing the opening of the flask in 5 cm depth in the surface snow. When the flask is full, the screw cap is carefully on-screwed again and the flask is stored in a refrigerator at 4 °C and in darkness until it is shipped to ENVS laboratory for analysis.

The analysis was carried out by concentrating the mercury samples on gold traps before analysing them with fluorescence spectroscopy. The detection limit is 0.4 ng L⁻¹ and the standard deviation on replicate analyses is between 6 and 9%.

3.5 DEHM model

The Danish Eulerian Hemispheric Model (DEHM) (21, 22) is a 3D atmospheric chemistry-transport model. The model domain covers the Northern Hemisphere using a polar stereographic projection with a grid resolution of 150 km x 150 km. It includes nesting capabilities to make simulations with a higher grid resolution in a limited area of the domain. DEHM includes four chemical groups: a group with SO_x-NO_x-VOC-ozone chemistry (71 components in total including secondary organic aerosols SOA), a group with primary particulates (9 components including black carbon, primary organic aerosols and Pb), a mercury chemistry group, and finally a group with Persistent Organic Pollutants (3 HCH isomers, 11 PCB congeners and D5). The model is driven by meteorological data from a numerical weather prediction model, either the WRF model (the new version of the model system) or the MM5 model (only used for the model simulations including POP's). DEHM also applies emission estimates based on activity data as input. The set-up for the model simulations presented here has varied and will be described in the appropriate sections. DEHM has been applied to study atmospheric pollution in the Arctic for two decades (4, 21, 23-26). The activities at the Villum Research Station, Station Nord are vital for the development of new parameterization and for evaluating the DEHM model.

One of the most important inputs to the DEHM model system is the emissions. Emissions of the species to SO_x-NO_x-VOC-ozone chemistry and the particles are based on several inventories, including global emission databases, namely ECLIPSE V5.0 global emission for the years 1990, 1995, 2000, 2005, 2010 and 2015 on a 0.5°x0.5° (ref: see <http://www.iiasa.ac.at/web/home/research/researchPrograms/air/ECLIPSEv5.html>). The RCP (Representative Concentration Pathways) with a 0.5° x 0.5° resolution for historical data (27) was used to adjust the ECLIPSE for the years before 1990. Furthermore, emissions from the EMEP (European Monitoring and Evaluation Program) expert database, EMEP webdab version June 2016, with 50 km x 50 km resolution (ref: see http://www.ceip.at/ms/ceip_home1/ceip_home/webdab_emep-database/emissions_emepmodels/) was used for the Europe domain.

Several kinds of emission inventories are used for natural sources in the model system. Emissions from biomass burning are based on The Global Fire Assimilation System, GFA, (28) which is based on satellite measurement of surface temperature for the period after 2003 and the retrospective wildfire reanalysis, RETRO, before 2003 (29). The current version of DEHM includes the temporal allocation of emissions from the module of Emissions of Gases and Aerosols from Nature (MEGAN) (30, 31) as an in-line module. Natural emissions of NO_x from lightning and soil as well as emissions of NH₃ from soil/vegetation based on GEIA emission inventory are also implemented in the model.

The POP module is using several different emission inventories. The emission input for α-HCHs is monthly averaged emissions for 2000 (32), emissions for β-HCH are calculated as 1/6 of the emissions from α-HCH, and the emissions for γ-HCH are unpublished data from a personal communication by Yi-Fan

Li. The PCB emissions are annual emissions based on the high emission scenario from (33), which is the estimate that results in the best fit with observed concentrations.

The Mercury module are using Historical Global Inventories of Anthropogenic Mercury Emissions to Air made by AMAP (34) for the years 1990(v6), 1995(v6), 2000(v6), 2005(v6) and 2010(v1). Ocean fluxes of Hg are obtained from the GEOS-CHEM model (Personal communication, Anne Lærke Sørensen). Furthermore, emissions of Hg from biomass burning are included based on the biomass emissions of CO and a fixed Hg/CO ratio. The Lead emissions are based on the old global Lead inventory for the year 1989 (35). The emissions in all domains are distributed in time and with height above the surface following patterns depending on the source categories.

In this report, two different model setups and runs with DEHM have been performed. The first model run is with the POP group together with SO_x-NO_x-VOC-ozone chemistry (without SOA), where the MM5v3.7 weather forecast model (36) driven by global data from either ECMWFs TOGA/COARE dataset (before 2000) or NCEP operational analysis (after 2000), have been used as meteorological input to the model system. This DEHM model setup has been run for the whole period from 1989-2015.

The second model run is with at setup including SO_x-NO_x-VOC-ozone chemistry, primary particulates and mercury chemistry. The DEHM model was run for the whole period from 1979-2015. For this simulation meteorological data from the Advanced Research WRF version 3.6 (WRF ARW) (37) is applied. This WRF model simulation is driven by global meteorological ERA-Interim data, which is a global atmospheric reanalysis data set from the European Centre for Medium-Range Weather Forecasts (ECMWF) starting from 1979 and continuously updated in real time. These data have been nudged every 6 hour into the WRF model. The WRF model is run in a climate mode setup, e.g. continuously updating Sea Surface Temperature and deep soil temperature (both from the ERA interim).

4 Results and Discussion

4.1 Filter pack sampler results

The filter pack sampler results are separated into three different sections. The first section focus exclusively on sulphate-containing aerosols and the corresponding precursor sulphur dioxide. These species are responsible for a major part of the Arctic anthropogenic aerosol. In the second section we will discuss natural emissions in the Arctic and their trends. In the third section we will focus on selected elemental species that were analysed by the PIXE/ICP-MS and other techniques, which are known to originate from long-range transport from mid-latitudes reaching the Arctic as environmental contaminants.

4.1.1 Sulphate and Sulphur dioxide

In Figure 4.1 the monthly mass concentrations of sulphur dioxide and sulphate in units $\mu\text{g S m}^{-3}$ are presented over a period of 26 years. Sulphate and Sulphur dioxide have been measured by ion chromatography. The time series at VRS appears only with small interruptions except for the period from 2002 to 2007 when the location was closed and no data were available from VRS. The sulphate concentrations show a typical seasonal pattern which is characteristic for the appearance of Arctic haze at VRS. This phenomenon has been observed during previous studies for the same location (7, 10, 38), but for this investigation much more data is available compared to earlier studies.

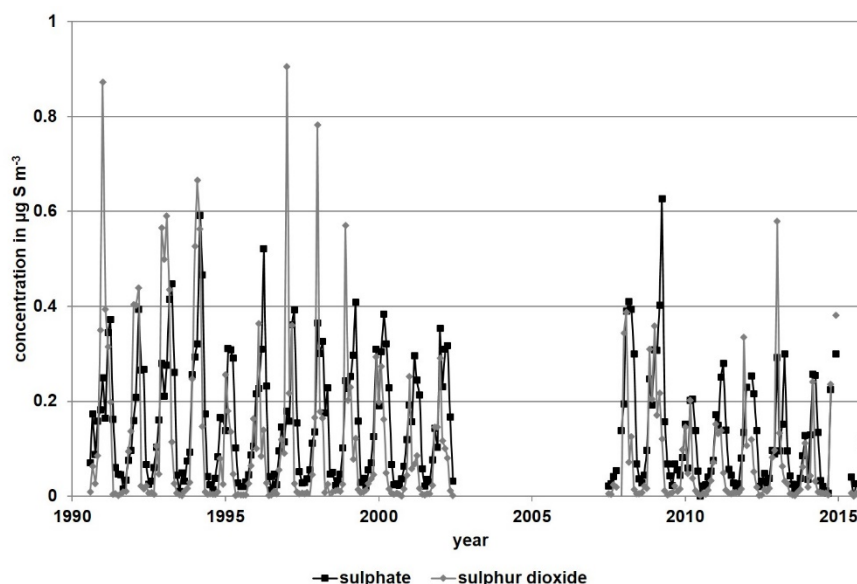


Figure 4.1. Time series of monthly mass concentrations of S in sulphur dioxide and sulphate measured at VRS in North Greenland during the observation period from 1990 to 2015.

It is well known that sulphur dioxide is a major precursor gas for the formation of sulphate aerosol. The emission of sulphur dioxide is related to both anthropogenic and natural sources. A major natural source is the oceanic emission of DMS (Dimethyl sulphide) which is oxidized to sulphuric acid via

sulphur dioxide. Sulphuric acid is a source for new aerosol particles. In a different process, sulphuric acid does also build sulphate aerosol by agglomeration with existing particles. The relative efficiency of these processes depends on the availability of surface concentration of particulate matter.

The concentrations of sulphur dioxide and sulphate both show a high variation over the years. In summer, the values are between 0 – 0.1 $\mu\text{g S m}^{-3}$, but in late winter and spring values of about 0.4 to 0.6 $\mu\text{g S m}^{-3}$ for sulphur dioxide and 0.4 to 1.0 $\mu\text{g S m}^{-3}$ for sulphate have been observed. In general, sulphur dioxide and sulphate concentrations show a similar pattern having a seasonal variation each year. This variation is slightly different comparing the two compounds and will be discussed in a following paragraph.

From Figure 4.1 it can also be seen that there is a slight decreasing trend in sulphur concentrations for both components over the years. The annual averages of the two components were therefore determined and the corresponding time series from 1990 to 2005 measured at VRS is presented in Figure 4.2.

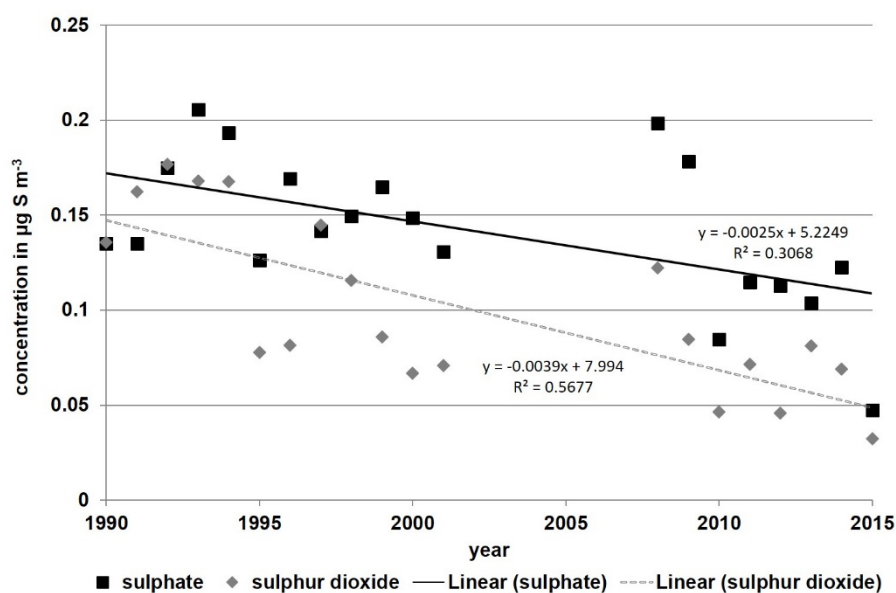
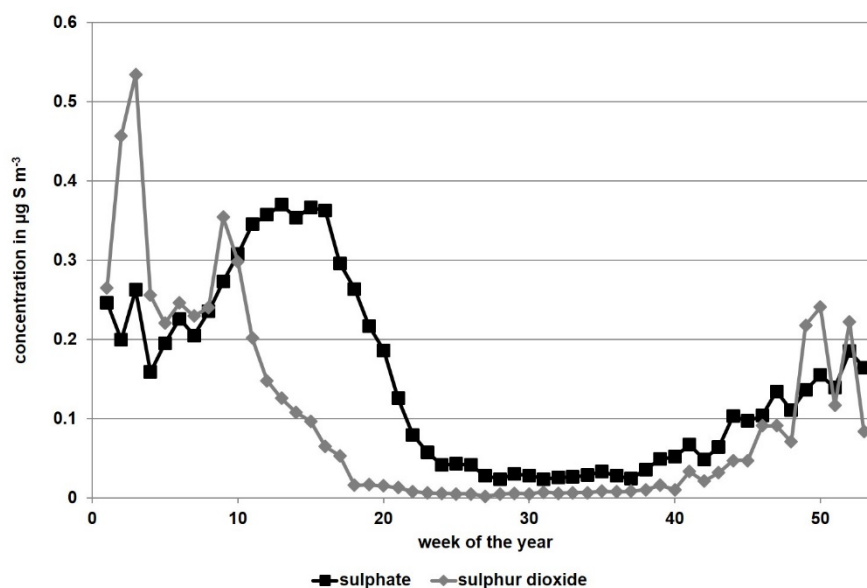


Figure 4.2. Trend of annually averaged mass concentrations of sulphur dioxide and sulphate measured at Villum Research Station, Station Nord in North Greenland during the observation period from 1990 to 2015.

In general, sulphur dioxide annual averages vary from values of about 0.13 – 0.18 $\mu\text{g S m}^{-3}$ in the early nineties to 0.05 – 0.08 $\mu\text{g S m}^{-3}$ in the last five years. In comparison, sulphate concentrations show slightly higher variations for these periods. As the measurements were moved to Nuuk in 2002 to 2007 from VRS, the data representativity for these two particular years is very low. Data from 2002 and 2007 are not considered in this analysis (for 2002, data are mostly available for the beginning of the year (haze season) and for 2007 data are mostly available for the end of the year (early winter season) which may falsify conclusions). The trends observed in Figure 4.2 for sulphate and sulphur dioxide are significant on a 95 % confidence level.

A very high value in 2008 for both compounds can be explained by an overall extremely efficient transport of anthropogenic pollution particularly in the winter 2007/2008 based on a very strong Polar Vortex as discussed by Grube (2011)(39). In summary, a decreasing trend in yearly mean concentrations of sulphur dioxide and sulphate is observed from Figure 4.2 with regard to the linear regression. This corresponds to global regulations decreasing the sulphur content in fossil fuels to limit the emissions of sulphur dioxide and further formation of sulphate aerosols. However, these restrictions are limited to Western Europe. On the other hand, there are also rising emissions in Asia and South-east Asia, which can contribute to observations at VRS. It has to be stated that with global change and increasing Arctic temperatures, it is also expected that major atmospheric transport patterns will change. However, such changes are currently far from being quantified. Also, nowadays much more transport does happen over open waters, as the sea ice extent in summer is decreasing rapidly. All in all, observations at VRS are a result of various factors that have changed over time and a clear assignment of the decrease of sulphur dioxide and sulphate to different specific factors is currently not possible.

As observed in Figure 4.1, the sulphur dioxide and sulphate concentrations experience a seasonal variation. For this reason we analysed the seasonal variation by averaging the observed data to weekly values for the whole measurement period from 1990 – 2015. The results are presented in Figure 4.3.



Figur 4.3. Seasonal variation of weekly mass concentrations of S in sulphur dioxide and sulphate measured at Villum Research Station, Station Nord in North Greenland during the observation period from 1990 to 2015.

From Figure 4.3 it is clearly seen that sulphate concentrations reach their maximum values between the end of March and beginning of May (about week 12 to week 16) every year resulting in concentrations of up to $0.35 \mu\text{g S m}^{-3}$. In May and June mass concentrations show a dramatic drop to less than $0.1 \mu\text{g S m}^{-3}$. Minimum values are finally observed between July and September. As a major characteristic sulphate concentrations start rising slowly from October,

but the increase up to the maximum values is occurring over a much longer time period (about 6 months) compared to the observed decrease (about 2 months).

Analyzing the seasonal variation of sulphur dioxide concentrations for the time period between 1990 to 2015 presented as weekly averages in Figure 4.3 a slightly different picture is observed. Here, the monthly maximum is found in January given a value of about $0.5 \mu\text{g S m}^{-3}$ and the decrease to minimum numbers takes about four months (end of May) resulting in values lower than $0.02 \mu\text{g S m}^{-3}$. The increase in mass concentration for sulphur dioxide looks quite similar to the one discussed for sulphate except that sulphur dioxide concentrations peak earlier.

The observation of these patterns is in perfect agreement with the fact that sulphur dioxide is a precursor for sulphate and that the oxidation in the atmosphere is triggered by sunlight.

It can be concluded that the anthropogenic fraction of sulphur dioxide and sulphate is generally very high at VRS as sulphur dioxide originating from oceanic DMS is only expected in summer, where a larger amount of open waters could contribute to DMS emissions. As can be seen from Figure 4.3 the concentrations of sulphur dioxide and sulphate are very low in summer leading to the conclusion that the largest part of annually observed sulphur originates from long-range transport from mid-latitudes to the high Arctic.

In Figure 4.4 model results of sulphur dioxide (SO_2) and sulphate (SO_4^{2-}) from the second DEHM model setup run with SO_x - NO_x -VOC-ozone chemistry, primary particulates and mercury chemistry and with meteorological data from WRF as input, for the period 1990-2015 have been compared with the measured values at VRS. The figures show a very good performance of the DEHM model with a high correlation.

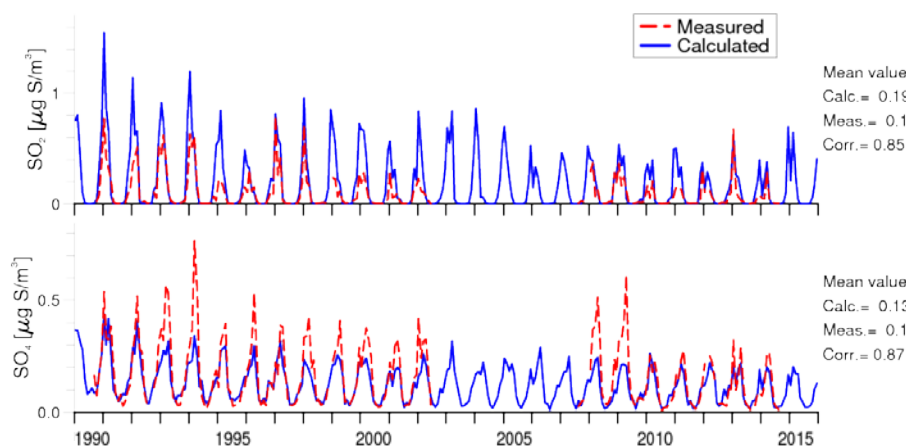


Figure 4.4. Calculated monthly concentrations of SO_2 and SO_4^{2-} in $\mu\text{g S m}^{-3}$ compared with the measured concentrations at VRS.

4.2 Natural sources

The section on natural sources in this report is subdivided in the following two sources, the first one originating from soil and the second one originating from the marine environment.

Soil source

In principle, only few natural primary sources of aerosol particles are located in the Arctic. These include the emission of soil dust, which is wind-blown and can only be observed during the snow-free season in summer when the dust is originating from Greenland in the vicinity of Villum Research Station. Most surfaces in Greenland are snow-covered all year round. On the other hand, smaller dust particles (around 1 μm in size) can be transported also over long distances. This way, crustal material from the Saharan desert can occasionally be observed in Central or Northern Europe and even at VRS depending on sufficient meteorological transport patterns. Also, it is well known that dust from the Saharan desert is transported over the South Atlantic Ocean to fertilize areas in South America. Components that are identified in and linked to soil dust are Al, Si, Ca, Ti, Mn, V, and Fe (10). On a global scale crustal material contributes second-most to particulate mass in the atmosphere and can have substantial climate effects with respect to its physical properties. This way, dust particles are known to function efficiently as ice nuclei affecting the indirect aerosol effect, to contribute to the direct aerosol effect because of their light absorbing potential or they can be deposited on snow- and ice-covered surfaces and change the surface albedo (40).

In Figure 4.5, the time series of the most abundant species Al and Fe for the period from 1990 to 2015 are displayed.

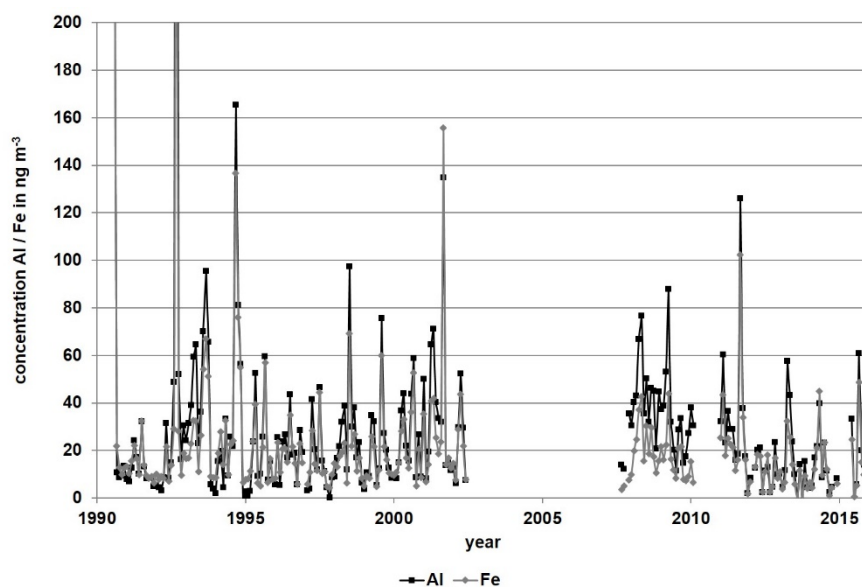


Figure 4.5. Time series of monthly mass concentrations of Al and Fe measured at VRS in North Greenland during the observation period from 1990 to 2015.

Mass concentrations of the selected species range from 5 - 10 ng m⁻³ to hundreds ng m⁻³ and more depending on the time of the year. A seasonal pattern can also be observed for all the species, which is not surprising having in mind that soil dust cannot be observed with equal abundance over the whole year as discussed above.

The trend of annual averages from 1990 to 2015 is presented for the selected species in Figure 4.6. Again, the data missing between 2002 and 2007 is due to the move of the measurement location from VRS, North Greenland, to Nuuk in Southeast Greenland.

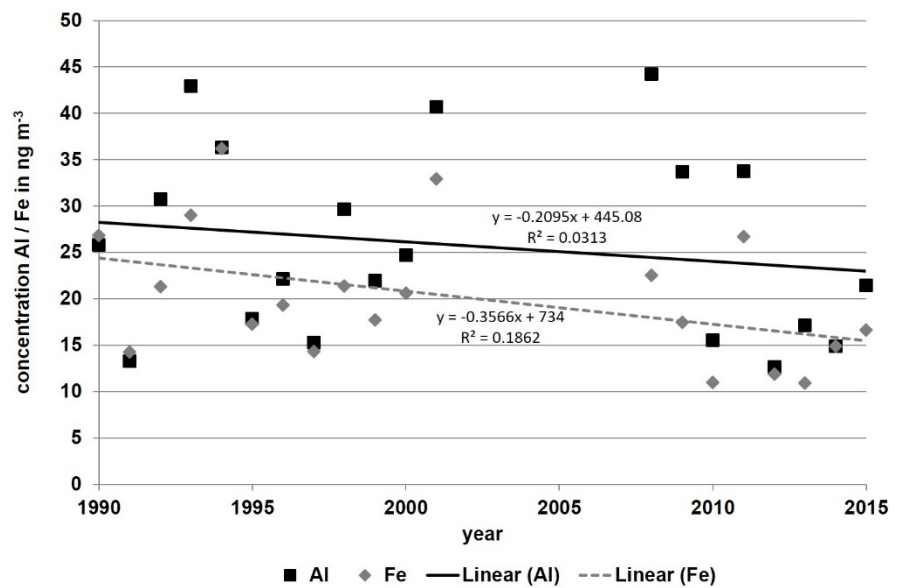


Figure 4.6. Trend of annual mass concentrations of Al and Fe measured at VRS in North Greenland for the observation period from 1990 to 2015.

In general, the annual averages of the selected species representing the soil dust as a natural source at VRS does not show a temporal trend that may indicate changes of this emission source in the Arctic based on a 95% confidence level. In general, it is difficult to deduce the reasons for a temporal trend, which is induced either by changing emissions, changing transport pattern or climatic changes. Larger areas without snow or ice cover and higher wind speeds induced by climate change might be a reason. However, such impacts or even feedback mechanisms of changing climate processes are far from been understood in detail today.

In order to get a clear picture of seasonal variations of natural soil dust emissions observed in the Arctic, the seasonal trend in weekly mass concentrations of the selected species is displayed in Figure 4.7.

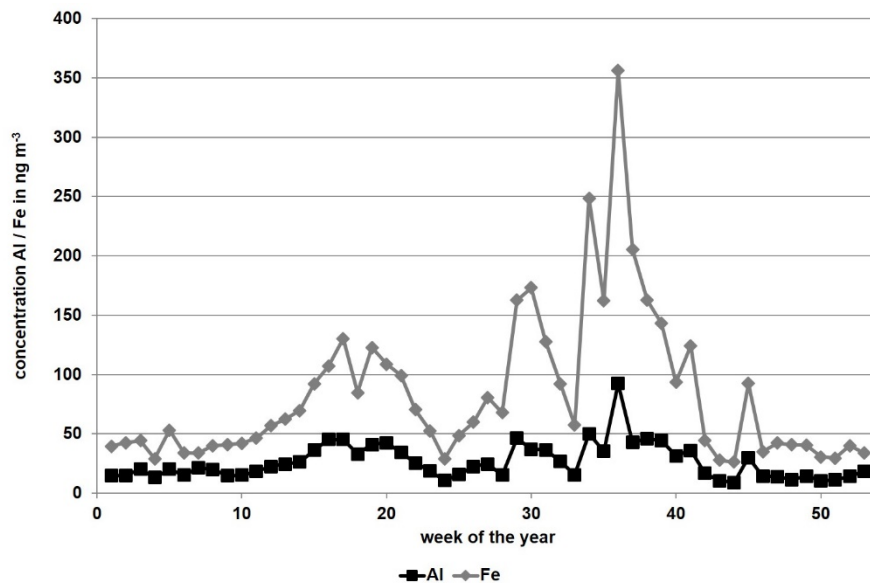


Figure 4.7. Seasonal variation of weekly mass concentrations of Al and Fe measured at VRS in North Greenland during the observation period from 1990 to 2015.

The weekly variation over the 52/53 weeks per year does show a clear seasonal pattern for the soil dust-related species. In general, mass concentrations peak about three times the year as in week 15 to 25 (May/June), around week 25 to 35 (June/July), and in week 35 to 45 (September/-October). The soil dust source is expected to be highly wind-driven and thus yearly wind patterns might explain these observations.

Marine Source

Marine emissions is another natural source of particles that is observed at VRS. The largest source contributing to aerosol mass worldwide is the emission of sea spray particles. Sea spray particles are a mixture of inorganic salts, but to some extent also organic material can contribute to sea spray particles (41). In general, sea spray emissions range in sizes between few hundreds of nano-meters to several micro-meters. As the inorganic and most abundant compound is sodium chloride the time series of sodium and chlorine observed at VRS over the time period from 1990 to 2015 is displayed in Figure 4.8.

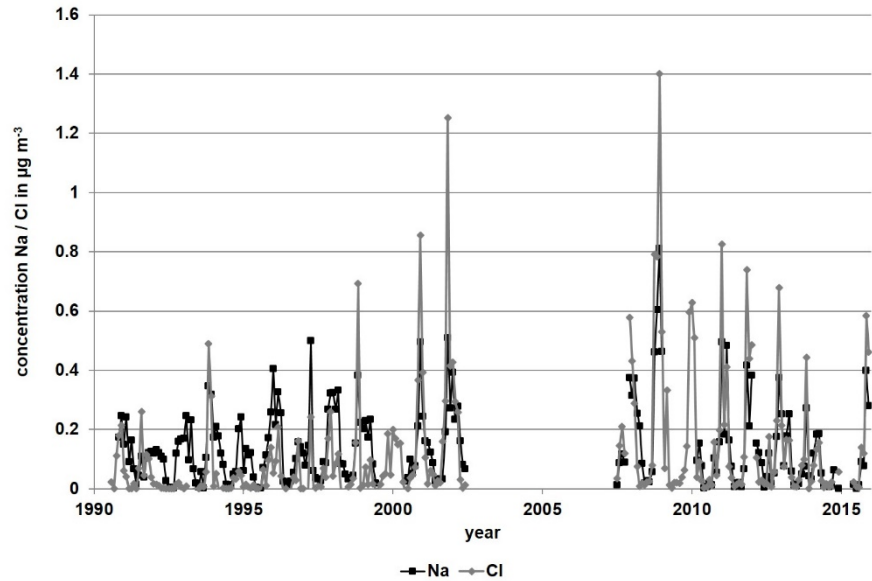


Figure 4.8. Time series of monthly mass concentrations of Na and Cl measured at VRS in North Greenland during the observation period from 1990 to 2015.

From Figure 4.8 it can be seen that both species show a seasonal pattern; this is investigated in more detail in a later section. In principle, monthly sodium concentrations range from tens of ng m^{-3} up to one $\mu\text{g m}^{-3}$. In comparison, chlorine concentrations show corresponding values on the same order of magnitude. Nevertheless, Figure 4.8 suggests that the molar ratio of sodium to chlorine has been changing between 1990 and 2000 and 2000 to 2015, which might be caused by a more efficient detection of chlorine with the IC method in the second period. For this reason, care has to be taken when making conclusions on changing emission patterns e.g. caused by more open waters throughout the latter period affected by climate change.

To investigate if there is any temporal trend in sea spray particles, the annual averages of the two species representing the marine aerosol source at VRS are presented in Figure 4.9.

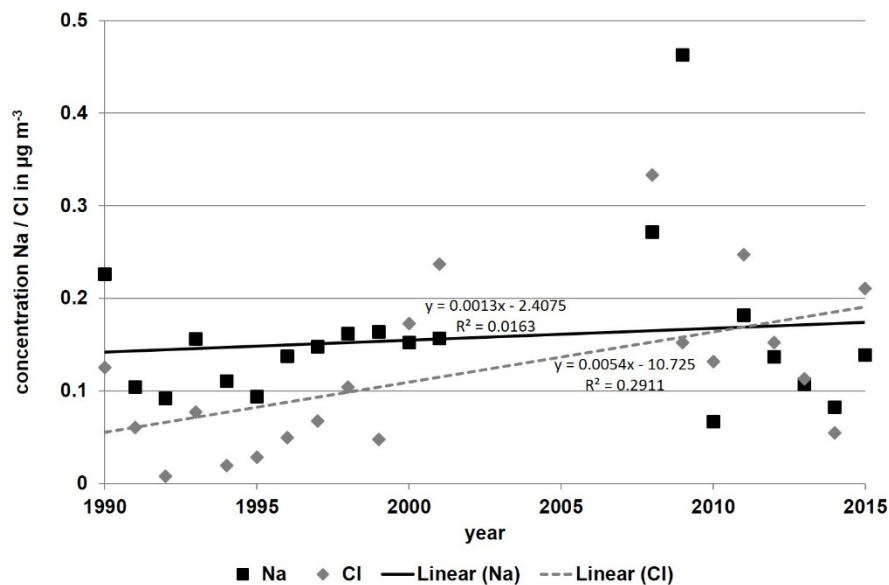


Figure 4.9. Trend of annual mass concentrations of Na and Cl measured at VRS in North Greenland for the observation period from 1990 to 2015.

The annual averages for sodium and chlorine show relatively large variations over the measurement period from 1990 to 2015. A general trend in terms of increasing values is only significant for chlorine on a 95 % confidence level. At the same time, the detection efficiency has to be considered after 2000 due to the change in analytical method. Therefore conclusions on an emission change cannot be drawn. This finding is similar to what was found for the soil dust source and not surprising either. Also for the marine source, a change in emissions based on climate changes is difficult to quantify. Nevertheless, as the area of open seawaters has been dramatically increasing during the observation period from 1990 to 2015, an increase in sea spray emissions is expected, but probably not detectable here as longer time series or a more detailed analysis of Arctic wind patterns and their spatial resolution is needed. The identification of such changes would be understood as one important feedback mechanism driving climate change. A detailed view in the seasonal variation of the inorganic marine-related species is given in Figure 4.9. For this investigation data were averaged for the respective week numbers 1 to 52/53 over the whole measurement period from 1990 to 2015 as done for other species and discussed above.

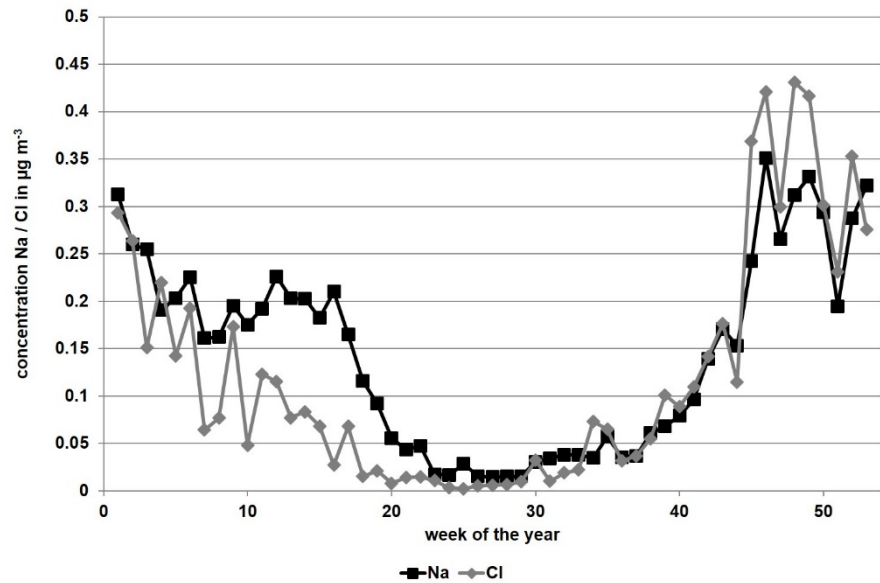


Figure 4.10. Seasonal variation of weekly mass concentrations of Na and Cl measured at VRS in North Greenland averaged during the observation period from 1990 to 2015.

Similar to the soil dust source, the marine source shows a clear seasonal pattern, but in contrast, this pattern has a much simpler structure. A clear minimum in concentration is observed in week 20 to week 35 (June to September) identifying the summer and early autumn period at VRS in North Greenland. The summer sea ice minimum in the Arctic appears in September each year, which can clearly be determined from satellite imaging. A minimum of sea ice in combination with sufficient wind speeds results in a maximum of sea spray emissions. This rise in emissions can be seen in Figure 4.10 as sodium and chlorine concentrations obviously increase in October shortly after the appearance of the sea ice minimum when the open water maximum is reached in the Arctic. The concentrations peak by the end of the year, which is the time when the waters start to freeze again. The seasonal pattern of the marine sea spray emissions is not only linked to cryospheric processes but is also strongly linked to the meteorological conditions as the production of sea spray particles is highly dependent on the wind speed and also on the salinity of the oceanic water. Based on source to receptor modelling which has been carried out by Nguyen et al. 2013 (10) using a dataset of 3 years from 2008 to 2010, sodium as well as chlorine are species which can largely be linked to natural sources at VRS. An additional source to sodium and chlorine can also be biomass burning that can be either of natural or of anthropogenic origin while the largest part is typically anthropogenic. An additional natural source for the species is frost flowers that occur from refreezing leads (42).

In Figure 4.11, sea salt calculations obtained from the second DEHM model setup for the period 1990-2015 have been compared with the measured values at VRS. The performance of the DEHM model is not as good as for sulphur dioxide and sulphate. This is mainly due to much higher uncertainties in the calculated fluxes of sea salt, which are dynamically calculated inside the DEHM model based on the 10 m wind speed and salinity. The very low levels of sea salt at VRS are furthermore connected with high analytical uncertainty.

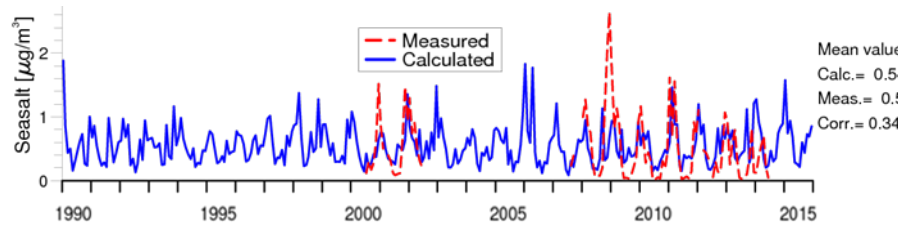


Figure 4.11. Calculated monthly concentrations of sea salt ($\mu\text{g m}^{-3}$) compared with the measured concentrations (based on Na contents in sea salt) at VRS.

4.2.1 Anthropogenic sources

The section on anthropogenic sources of aerosol particles will be subdivided into the following two sources, the first one predominantly originating from smelters in Northern Russia emitting metals as Cu and Ni containing material and the second one originating from combustion processes.

Metal source (Cu/Ni)

It is well known that during the late winter and the early spring long-range transported aerosols reach regularly the high Arctic areas. The special meteorological conditions during this time of the year favour the transport of air masses from mid-latitudes to the Arctic and high Arctic. The pollution levels are mainly caused by anthropogenic activities. Nguyen et al. (2013) (10) found increased levels of Cu and Ni in Arctic aerosols observed at VRS that were assigned to the emission of Cu and Ni smelters. These smelters are located in Northern Russia, namely the Kola peninsula and Norilsk in Northern Siberia (7, 21, 38). The time series of the two species analysed on filter samples from 1990 to 2015 at VRS is shown in Figure 4.12.

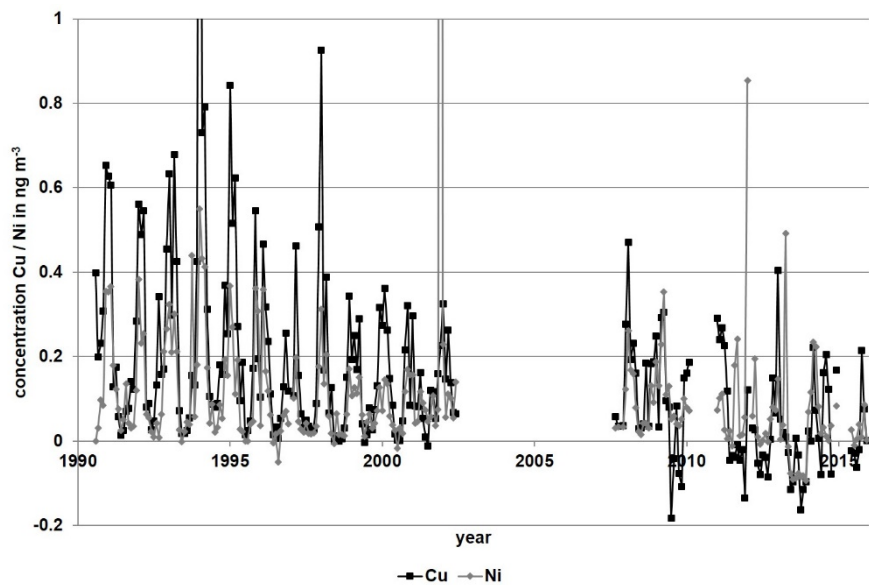


Figure 4.12. Time series of monthly mass concentrations of Cu and Ni measured at Villum Research Station in North Greenland during the observation period from 1990 to 2015.

In general, Cu and Ni mass concentrations range from few tens of pg m^{-3} to few hundreds of pg m^{-3} for both elements. These concentrations seem to be very low compared to pollution levels in Arctic areas in general and especially to pollution levels of particulate matter at mid-latitudes. Nevertheless, the sensibility of the Arctic environment has to be considered as e.g. the contamination of the food chain is a rising issue.

Annual averages of Cu and Ni mass concentrations are presented in Figure 4.13 in order to investigate if any annual trends can be observed throughout the last 25 years.

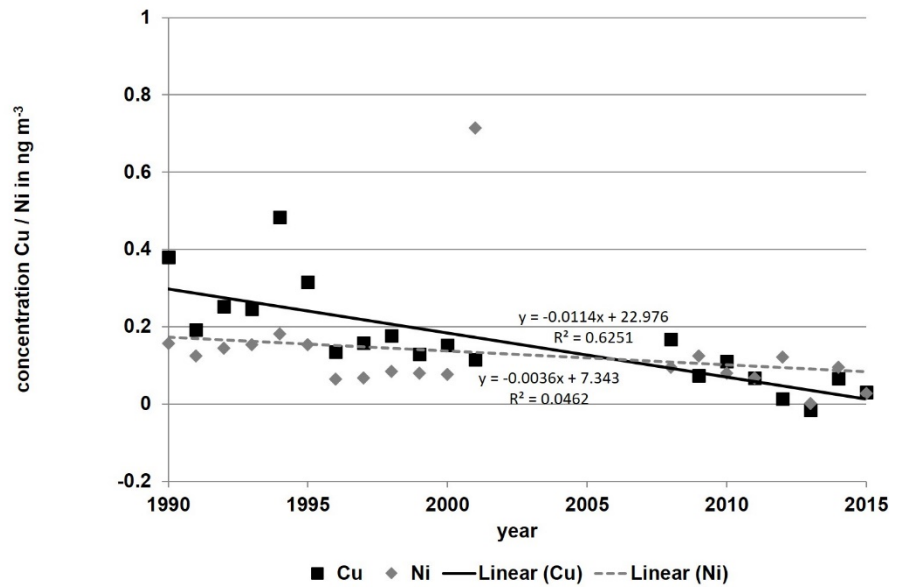


Figure 4.13. Trend of annual mass concentrations of Cu and Ni measured at VRS in North Greenland for the observation period from 1990 to 2015.

From Figure 4.13 a slight decrease in annual concentrations of both species, Cu as well as Ni, can be seen. Based on the 95 % confidence level, this decrease is significant for Cu, but not for Ni. As annual concentrations range between 0.2 to 0.5 ng m^{-3} for Cu and between 0.1 to 0.2 ng m^{-3} for Ni in the early nineties, these values dropped down to about less than 0.2 ng m^{-3} for Cu and less than 0.1 ng m^{-3} for Ni in the last five years. This tendency might be due to a reduction in the activities at the smelters in Northern Russia, but it can also be a result of changing transport patterns in the Arctic as a consequence of Arctic climate change and thus a result of so-called climate feedback mechanisms.

In Figure 4.14 a detailed view into the seasonal variation of Cu and Ni concentrations is shown as concentrations averaged for each week from week 1 to week 52/53 for all years when measurements were available in the period from 1990 to 2015.

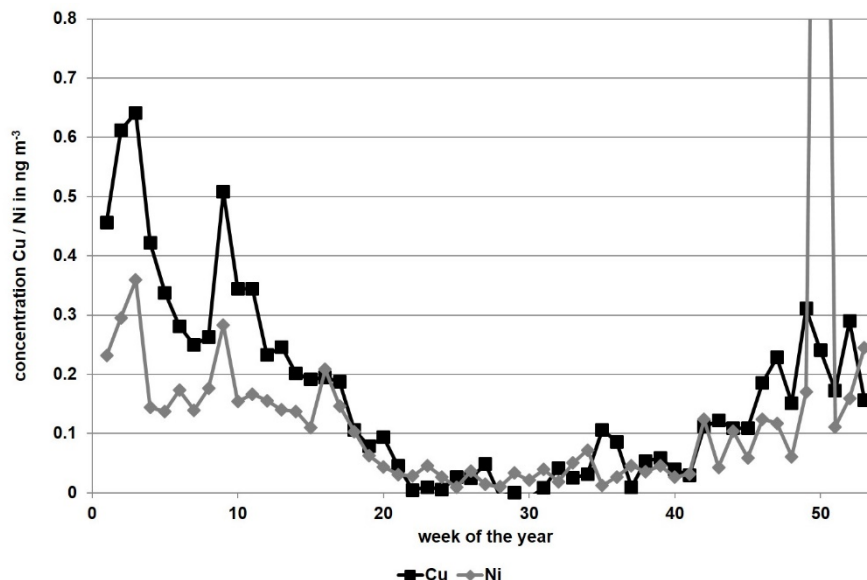


Figure 4.14. Seasonal variation of weekly mass concentrations of Cu and Ni measured at VRS in North Greenland averaged during the observation period from 1990 to 2015.

Again, as for the sulphur concentrations discussed in a previous section, a clear seasonal pattern is observed for the Cu and Ni sources that relates to the general anthropogenic transport pattern of aerosols reaching the high Arctic area between late winter and early spring each year. This behaviour is very typical and describes the pattern that is observed during the so-called Arctic haze. Having in mind that the activity at the smelters in Northern Russia is expected to be more or less constant over the yearly cycle; the efficiency in anthropogenic transport is evidently indicated by the rise and drop of concentration values around November and May each year.

Combustion source

A major and probably the largest source due to anthropogenic activities is the combustion of fossil fuels and possibly wild fires that are anthropogenically initiated. Typical emissions from these sources include species as Pb and As, but also Se and V (10). In addition, combustion processes are typically related to larger amounts of sulphur dioxide emissions that is a precursor for sulphate as discussed in a previous section. The time series measured throughout the period from 1990 to 2015 at VRS for Pb and As is displayed in Figure 4.15 representing the overall combustion source.

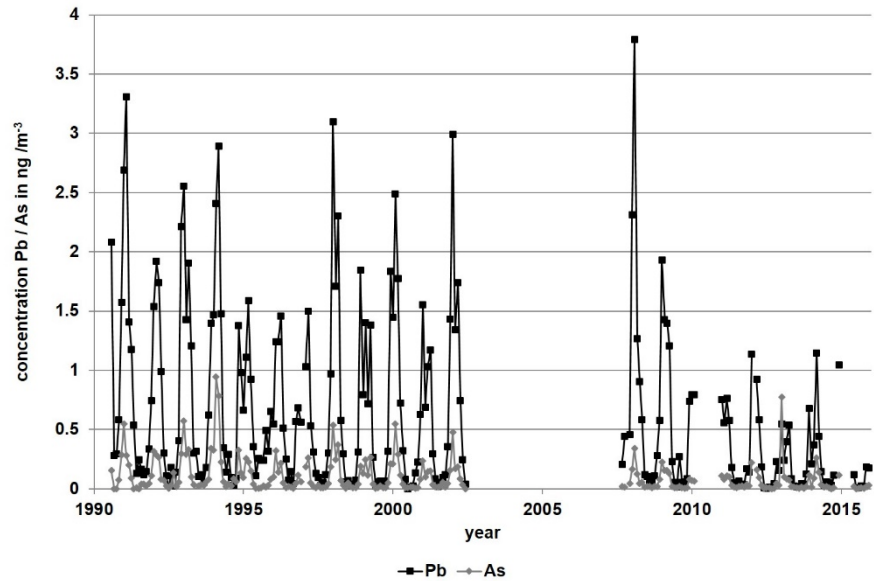


Figure 4.15. Time series of monthly mass concentrations of Pb and As measured at VRS in North Greenland during the observation period from 1990 to 2015.

From Figure 4.15 it can be concluded that monthly mass concentrations of e.g. Pb reach much higher values compared to those observed for typical Cu/Ni sources discussed in the previous section. Here, mass concentrations reach values up to 3 ng m⁻³ during certain periods of the year. Similarly as for the Ci/Ni source, a decreasing tendency can be observed for Pb and As, which are here displayed in Figure 4.16 as a proxy for all other combustion-related species.

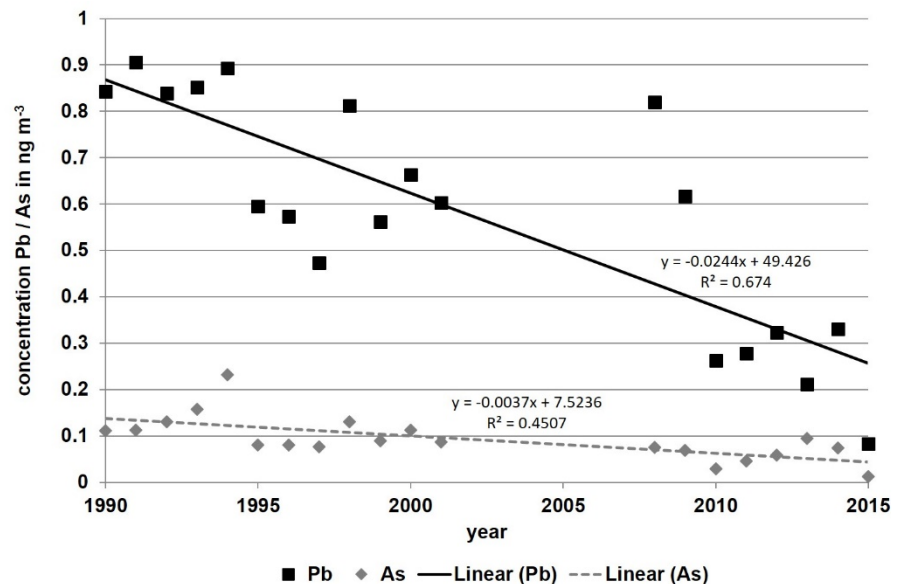


Figure 4.16. Trend of annual mass concentrations of Pb and As measured at VRS in North Greenland for the observation period from 1990 to 2015.

For Pb a strong decrease in annual concentrations is observed. A similar trend is observed for As but with much smaller gradient. For both species, the trend is significant based on the 95 % confidence level. This tendency can be explained by the change in composition of fuels, a change to modern engine

technologies in road traffic, and improved cleaning technology of flue gases in larger industries. However, these changes are mostly evident for western European societies. The strong decrease in Pb is most likely linked to the regulated banishment of Pb in the combustion fuels in Europe. To which extent the observation of combustion-related species at VRS is affected by European and Asian (South-East Asian) emissions remains an open question.

In Figure 4.17 the seasonal variation of Pb and As is presented in order to identify the impact of anthropogenic transport of emissions from mid-latitudes to the high Arctic. As for the Cu/Ni source, combustion aerosols are also constantly emitted over the year, such that any pattern observed at VRS is meteorologically affected.

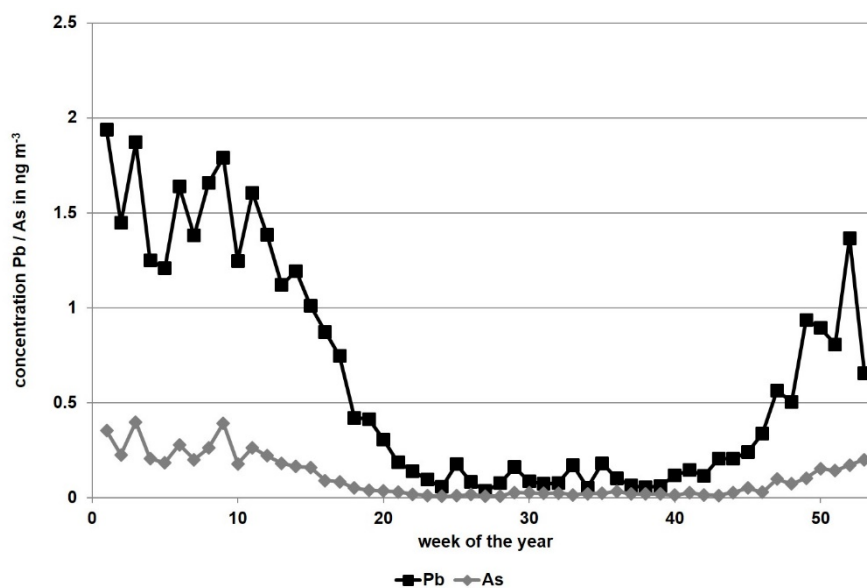


Figure 4.17. Seasonal variation of weekly mass concentrations of Cu and Ni measured at VRS in North Greenland averaged during the observation period from 1990 to 2015.

The pattern observed in Figure 4.17 in terms of shape is very similar to the one observed for the Cu/Ni source and underpins that mass concentration levels are particularly originated from sources outside the Arctic as values during the summer period are close to the general detection limit of these species.

In Figure 4.18 the monthly mean concentrations of Pb calculated by DEHM are compared with the measured concentrations. Again, the model is able to simulate the measured concentrations. Not surprisingly the model overestimates the measured levels in the last part of the period as the model is using a Pb emission inventory for 1989 (including lead in the gasoline) for the whole period as it is the only available global inventory for Pb (7). The measurement/model ratio is changing from 1.28 in 1991-1993 to 0.42 in 2012-2014, i.e. the ratio has decreased by a factor of 3.1 due to Pb emission reduction.

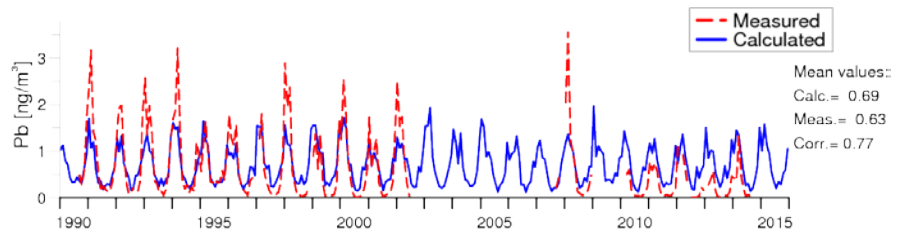


Figure 4.18. Calculated monthly mean concentrations of Pb in ng m^{-3} compared with the measured concentrations at VRS.

4.3 Modelling 37 years of Sulphate and Sulphur dioxide

A model simulation has been performed with the DEHM model system that covers the period from 1979 to 2015. This simulation was carried out using the second DEHM setup with SO_x - NO_x -VOC-ozone chemistry including SOA, 9 particulates, mercury chemistry and with the use of meteorological data from the WRF model as input.

The sulphur dioxide and sulphate concentrations in the Arctic have been evaluated by comparing with measurements from VRS for the period from 1979 to 2015 (Figure 4.19).

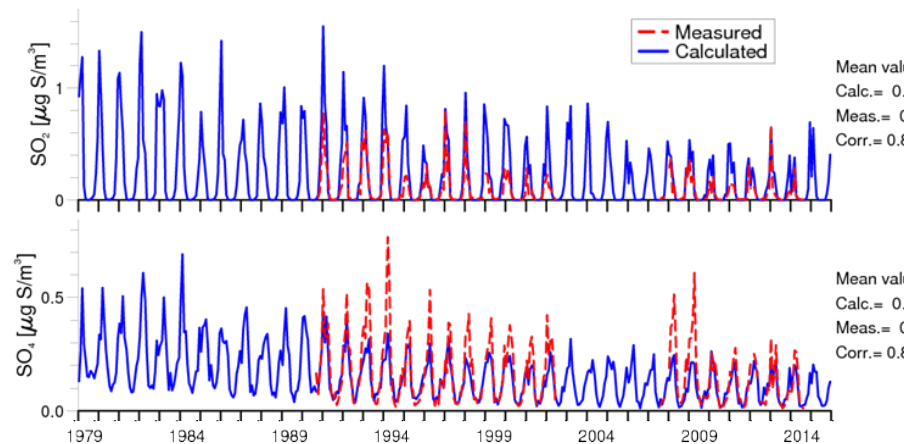


Figure 4.19. Calculated monthly concentration of sulphur dioxide (SO_2) and sulphate (SO_4^{2-}) in $\mu\text{g S/m}^3$ compared with the measured concentrations at Villum Research Station.

The simulated sulphur dioxide and sulphate concentrations generally agree well with the measured concentrations with an overall positive bias for sulphur dioxide and negative bias for sulphate. The overall averages agree well and the variability is well described with a high correlation coefficient ($r = 0.85$ for Sulphur dioxide and $r = 0.87$ for sulphate).

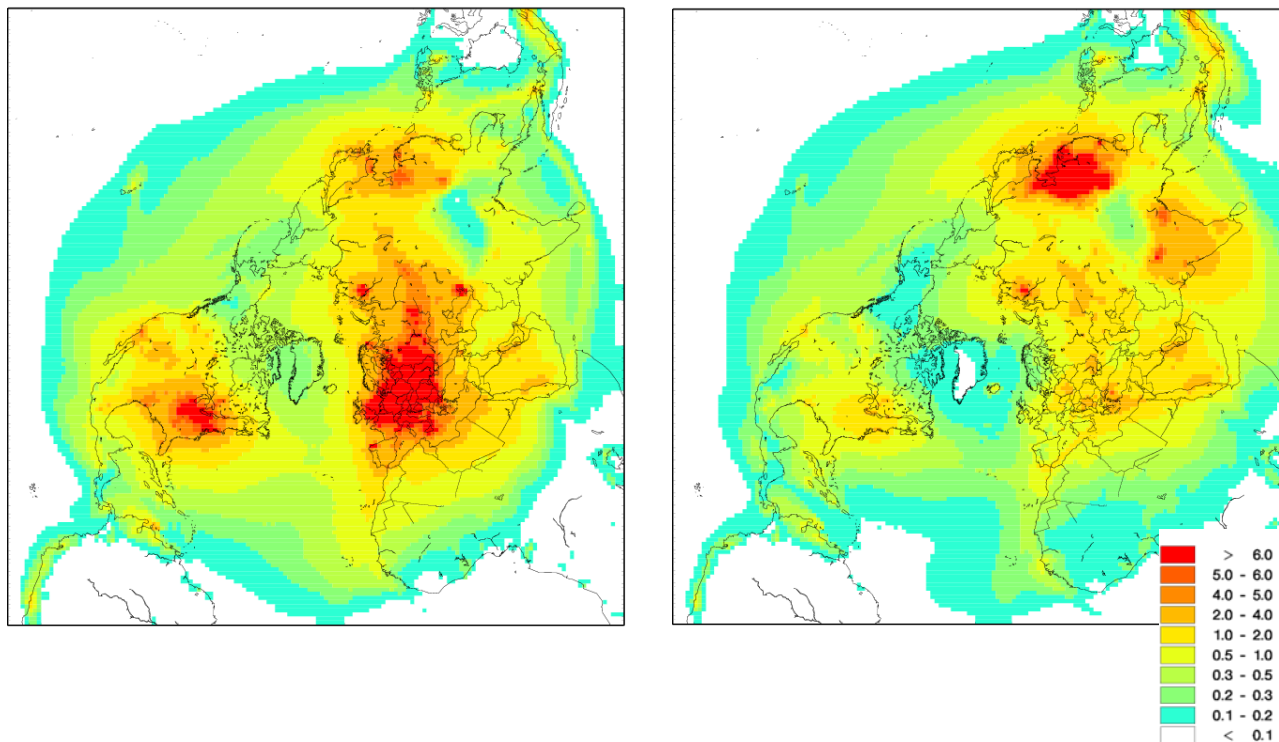


Figure 4.20. Simulated annual averaged concentrations of SO_x (=SO₂+SO₄²⁻) in µg S/m³ in 1979 (left) and in 2015 (right).

The concentrations are in general highest over source areas (North America, Europe and Asia), see Figure 4.20, but it is evident that SO_x is subject to long range atmospheric transport to remote areas as the Arctic. The concentrations decrease in most of the model domain, except over Southeast Asia and India.

Surface concentrations have been extracted for VRS, Svalbard and four other IASOA sites: Alert in Nunavut, Canada, Barrow in Alaska, USA and Tiksi and Cherski in Russia. The normalized annual averaged concentrations are illustrated in Figure 4.21.

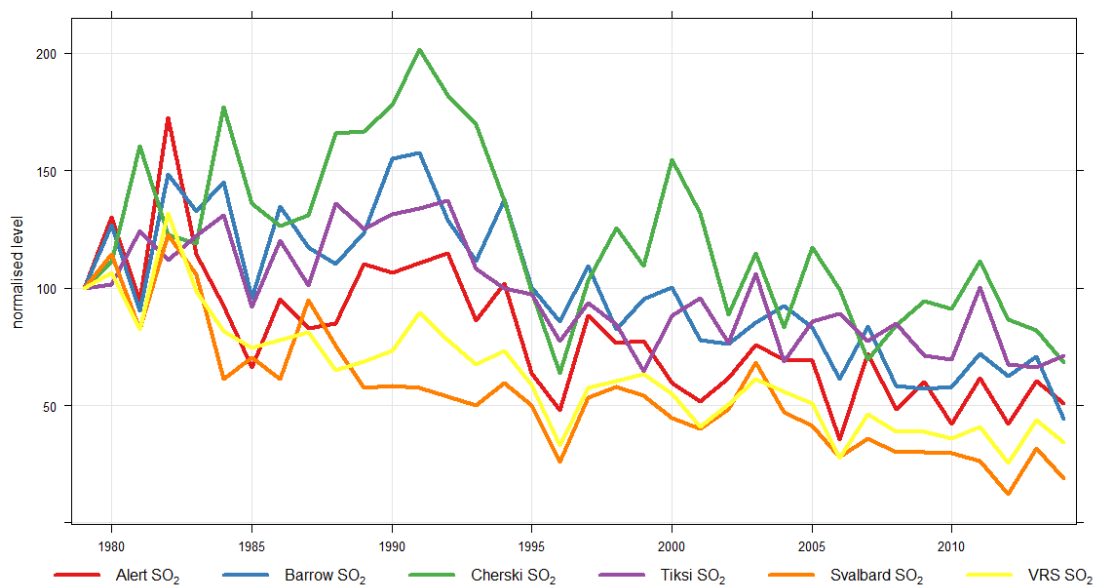


Figure 4.21. Simulated annual averaged concentrations normalized to the concentrations in 1979 from Alert, Nunavut, Canada (red), Barrow, Alaska, USA (blue), Cherski, Russia (green), Tiksi, Russia (purple), Ny Aalesund, Svalbard (orange) and Villum Research Station (yellow).

The annual averaged concentrations decrease at all sites, but not to the same extent. The largest decrease is observed at Svalbard (~75%), followed by VRS (~60%), Alert and Barrow (~50%) and the two Russian sites with ~35%.

Emissions in different source regions have been analysed to identify the origin of the difference in concentration development for the 6 studied sites within the Arctic. The total sulphur dioxide emissions (which is also a precursor for sulphate) within the model domain have been reduced with 40 % by the end of the model simulation compared to 1979 (Figure 4.22). The emissions from the European/African part of the domain have been reduced with 75 %, the emissions from the North American part have been reduced with 60 %, while the emissions from the Asian part have been increased with 35%. The increase in Asia is due to increasing emissions in Southeast Asia in general and in China in particular.

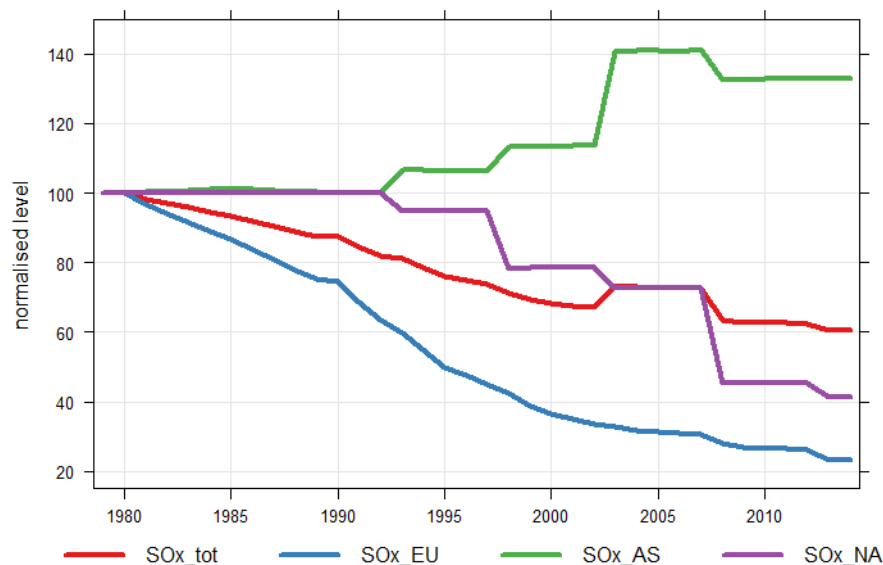


Figure 4.22. Annual averaged emissions applied in the model simulation normalized to the emissions in 1979. Total emissions (tot) in red, emissions from Europe/Africa (EU) in blue, from Asia (AS) in green and from North America (NA) in purple.

It can be seen that the decrease in concentrations at Svalbard, VRS, and to some extent Alert closely follows the decreasing emissions from Europe. This can be explained by the position of the polar front that on average extends into Europe in winter, so sulphur dioxide from Eurasia is emitted directly into the polar air mass and thus is easily transported to the Arctic sites. A similar close connection between the trend in concentrations and the emission in the nearest source area is not found for the other Arctic sites, where the locations are under influence of other sources than the European. Further studies will look into the relationship between sulphur dioxide and sulphate.

4.4 Results from High Volume Sampler

4.4.1 Organochlorine pesticides (OCPs)

Atmospheric concentrations both gas phase and particulate phase of the analysed OCPs in the period 2008-2015 are summarized in Table 4.1. One weekly sample was available for each month from 2008 to 2015, with the exception of years 2009, 2011 and 2013, where the number of samples was reduced to seven, eight and ten because of technical problems with the high volume sampler. No attempt to distinguish between gas phase and particulate bound compounds has been made since the sampler and part of the sampler inlet were kept at room temperature and thus particle/gas phase distribution of the compounds in the sample does not reflect the distribution in outdoor air.

Table 4.1. Average, median and concentration ranges (pg m^{-3}) of OCPs (pg m^{-3}) in years 2008-2015 (sum of gaseous and particulate phase) at VRS. Samples below the detection limit were assigned half of the detection limit value. The values are given only for those compounds detected in more than 30 % of the samples

Compound	Average	Median	Range
HCB	83.7	83.9	1.14-223
α -HCH	9.06	8.21	0.15-33.3
γ -HCH	1.32	1.09	0.07-11.8
Heptachlor	0.10	0.06	0.003-1.14
Heptachlor epoxide	0.58	0.55	0.02-1.49
Aldrin	0.01	0.003	0.003-0.20
Dieldrin	1.31	1.07	0.09-17.0
trans-Chlordane	0.24	0.21	0.02-1.03
cis-Chlordane	0.57	0.56	0.01-1.49
o,p'-DDT	0.27	0.20	0.02-4.04
p,p'-DDT	0.40	0.24	0.001-5.85
o,p'-DDE	0.05	0.04	0.001-0.17
p,p'-DDE	1.30	0.51	0.07-24.3
o,p'-DDD	0.20	0.07	0.05-6.22
p,p'-DDD	0.21	0.09	0.004-6.18
α -Endosulfan	2.97	2.57	0.04-14.1
β -Endosulfan	0.06	0.003	0.003-0.62
trans-Nonachlor	0.40	0.37	0.04-1.59
cis-Nonachlor	0.06	0.05	0.05-0.16

OCPs concentrations at VRS have been reported previously for the period 2008-2010 (3) and recently updated to 2013 (43).

The compound with the highest measured concentrations is hexachlorobenzene (HCB) with an average concentration of 83.7 pg m^{-3} and a range from 1.14 to 223 pg m^{-3} . Atmospheric concentrations measured from 2000 to 2005 at Alert (Canadian Arctic) and Zeppelin (Svalbard) varied from yearly average of 29 to 72 pg m^{-3} , so the present data set is at the high end for Arctic sites but comparable with values obtained at the two other high Arctic stations (8). HCB concentrations showed a weak seasonality at VRS, with slightly higher concentrations in summer.

The average annual concentrations of α -HCH and γ -HCH were 9.06 and 1.32 pg m^{-3} , respectively. The other isomers, β -HCH and δ -HCH, were only sporadically detected at very low concentrations. Seasonal variations were observed for α -HCH and γ -HCH. Higher α -HCH concentrations were observed from August to November, while γ -HCH concentrations were lower in the warm season (from May to August) and higher from September through the winter season.

α -Endosulfan was detected in all samples until 2013, while in 2014 and 2015 the compound was detected in 23 over 26 samples (average: 2.97 pg m^{-3}). β -endosulfan was only detected in 1/3 of the samples (average: 0.06 pg m^{-3}). The degradation product endosulfan sulphate was only sporadically detected with a frequency below 30 %. A seasonal pattern is observed for α -endosulfan

in the atmosphere characterized by elevated concentrations in April-May and again in September-October.

The two main components of technical chlordane, the stereoisomers *trans*-chlordane (TC) and *cis*-chlordane (CC) are detected in all samples with average concentrations of 0.24 and 0.57 pg m^{-3} , respectively. These values are comparable to those measured at Alert and Zeppelin in 2000-2006 (8). Technical chlordane also contains trace amounts of heptachlor, *trans*-nonachlor (TN) and *cis*-nonachlor (CN). TN and CN are detected at average concentrations of 0.40 and 0.06 pg m^{-3} , respectively. Heptachlor has also been manufactured on its own as an insecticide and the degradation product, heptachlor epoxide, is detected in all samples with an average concentration of 0.64 pg m^{-3} . Concentrations of all chlordane-related compounds showed seasonal variation, with relatively higher concentrations in the periods April-June and August-October.

Among DDTs and transformation products, *p,p'*-DDE (mean: 1.3 pg m^{-3}) was the most abundant compound, followed by *p,p'*-DDT and *o,p'*-DDT (mean: 0.40 and 0.27 pg m^{-3} , respectively). The average annual ratio *p,p'*-DDT/*p,p'*-DDE was 0.31, which indicates that DDTs have aged when arriving at these latitudes (44). The seasonal profile of *p,p'*-DDT showed a clear peak in June followed by a rapid decrease in July-August.

Dieldrin is detected in all samples with an average concentration of 1.31 pg m^{-3} . Aldrin was detected in about 30 % of the samples with a higher detection frequency in the last two years, while endrin is detected in very few samples and mostly close to the detection limit.

The temperature dependence of OCP concentrations is calculated for years 2008-2015 using the Clausius Clayperon (CC) equation. The slope of the logarithm (log) of the concentration versus reciprocal temperature ($1/T$) has been used to interpret the relative importance of volatilization from local sources versus long-range transport (45, 46). A statistically significant relationship at 95 % confidence level between log C and $1/T$ with a negative slope indicates that re-volatilization is an important mediating factor for the atmospheric concentration of a compound. The statistical results of the linear correlation of the measured concentrations of OCPs with temperature, following the Clausius-Clapeyron equation, are listed in Table 4.2. The parameters used for calculating the t-values were obtained using the function LINEST in Excel.

Table 4.2. Temperature dependence of concentrations of OCPs obtained with the Clausius-Clapeyron (CC). The following parameters are shown: N = degree of freedom; R² =correlation coefficient; p value=significance at 0.05 level using Student's t-test.

Compound	N	R ²	Significance at 0.05 level
HCB	94	0.103	No
α -HCH	83	0.186	Yes
γ -HCH	73	0.008	No
Heptachlor epoxide	86	0.113	No
Dieldrin	86	0.354	Yes
trans-Chlordane	86	0.106	No
cis-Chlordane	86	0.00001	No
o,p'-DDT	82	0.185	Yes
p,p'-DDT	84	0.243	Yes
o,p'-DDE	82	0.017	No
p,p'-DDE	86	0.030	No
o,p'-DDD	82	0.308	Yes
p,p'-DDD	82	0.310	Yes
α -Endosulfan	83	0.005	No
trans-Nonachlor	59	0.246	Yes

In a previous study (3), we found a significant correlation with temperature for α -HCH, heptachlor epoxide, dieldrin, *cis*-chlordane and p,p'-DDT. The concentrations of the same compounds, with the exception of heptachlor epoxide, showed again a significant correlation with the temperature (Table 4.2). Moreover, we also found significant correlations for o,p'-DDT, p,p'-DDT, p,p'-DDD, o,p'-DDD and trans-nonachlor. These compounds have been banned in Northern Europe and North America. Thus, their concentrations at VRS cannot originate from these areas. This fact and the temperature correlation fits then very well with re-emission from previously contaminated surfaces.

Temporal trends of OCPs have been investigated in order to identify increasing/decreasing concentrations of these compounds in the period 2008-2015. Two-tailed t-test ($p > 0.005$) is applied in order to assess the significance of the trend in concentrations in the investigated period. It should be pointed out that, in order to determine the half-life and confirm the consistency of the trend, longer monitoring periods are needed (e.g. over 20 years).

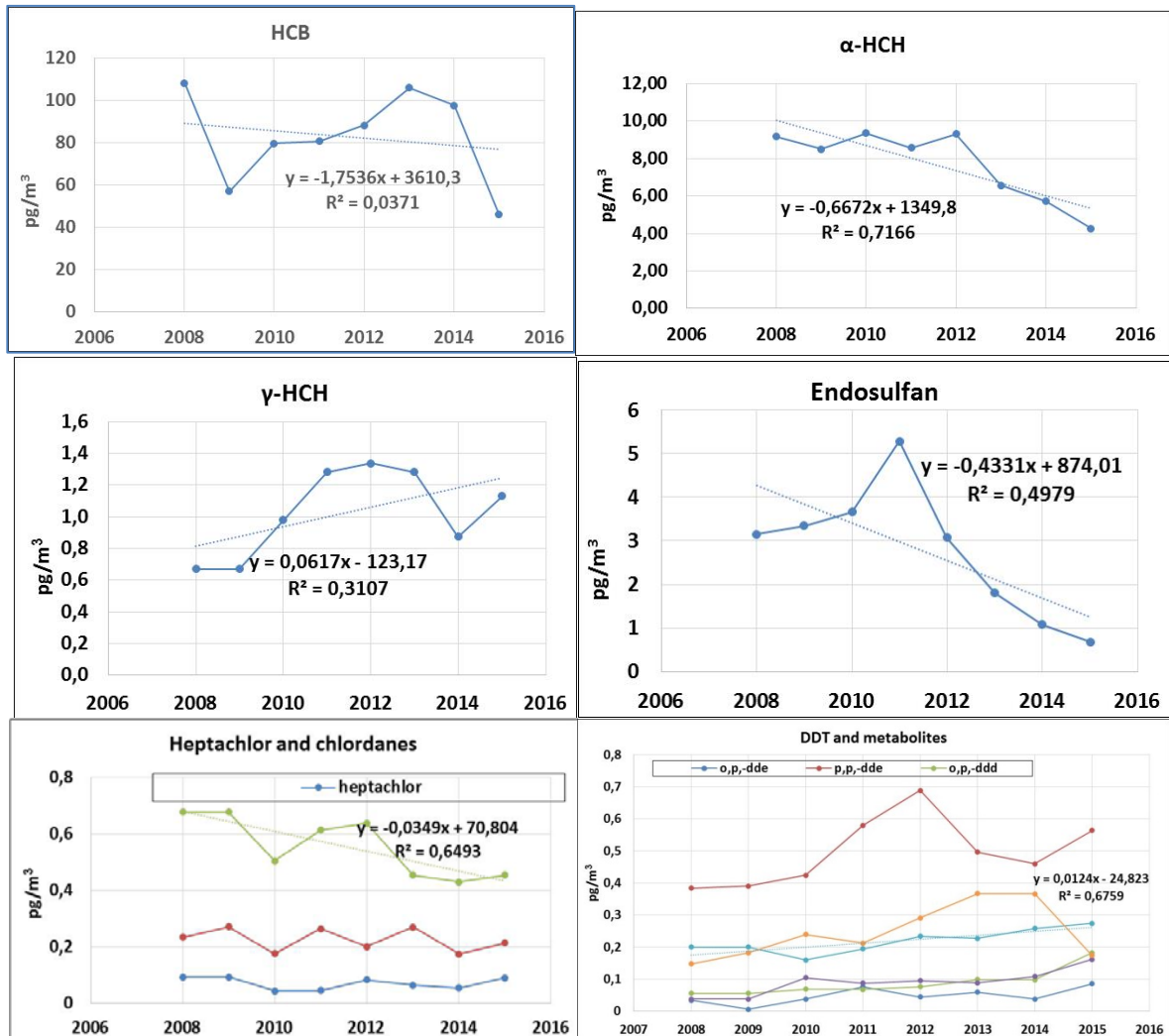


Figure 4.23. Temporal trends (2008-2013) of organochlorine pesticides. The median annual values have been used.

Significantly declining trends in atmospheric concentrations are observed for α -HCH, endosulfan and cis-chlordane on a 95% confidence interval, while significantly increasing trend is observed for o,p'-DDT and o,p'-DDD (Figure 4.20). Significantly decreasing concentrations have been observed for endosulfan after 2011. Atmospheric concentrations of endosulfan have also declined in 2011-2014 at two remote Canadian sites, which is consistent to the phase-out action in USA and Canada already started in 2010 (47). The peak in 2011 might be due to increased use of the pesticide stocks just before out-phasing. The contribution of long-range transported concentrations of endosulfan from Asia is also expected to decrease, since China has implemented the Stockholm Convention from March 2014 (48). The use of lindane (γ -HCH) has ceased worldwide and decreasing lindane concentrations have been observed at other Arctic sites (Alert, Stórhöfði, Pallas and Ny Ålesund) with half-lives between 4 and 7.3 years (49). This trend is still not evident at VRS and further years of monitoring will be needed. Slow or no declining trends are also observed at Alert for heptachlor, heptachlor epoxide, and DDT + metabolites (49).

4.4.2 Polybrominated flame retardants (PBDEs)

The atmospheric concentrations of PBDE congeners measured in the years 2008-2015 are summarized in Table 4.3. Only the congeners detected in more than 30 % of the samples are reported. BDE-209 was not included due to sporadic high levels of both laboratory and field blanks, which made it impossible, to correct the results for blank values. The \sum_{13} PBDEs concentration ranged from not detected (n.d.) to 6.26 pg m⁻³. The BDE congeners found in more than 30 % of the samples were BDE-17, BDE-28, BDE-47, BDE-71, BDE-99 and BDE-100. Compared with the composition of the commercial Penta-BDE mixtures DE-71 and Bromkal 70-5DE (50), the Arctic air samples are enriched in the most volatile congeners BDE-17 and BDE-28 and depleted in the remaining congeners. Interestingly, the samples from VRS also contain relatively more BDE-28 and less BDE-47 and BDE-99 than atmospheric samples from Nuuk (26). Besides differences in volatility, photochemical stability of the congeners will likely affect the PBDE composition, with BDE-99 being more susceptible to photolysis than BDE-47 and BDE-100 (51).

The average concentrations of PBDEs measured at VRS are about a factor ten lower than those measured at Alert (8, 44), but in the same range as other studies in West Greenland (52) and East Greenland (53). As suggested by the authors, the high BDE concentrations observed at Alert might have originated from direct emission from the local military station and the research station (8). BDE-71 was also detected in 58 % of the samples with an average concentration of 0.026 pg m⁻³. Very few studies have reported the presence of BDE-71 in atmospheric samples; Yu et al. (2015) (54) recently reported an average BDE-71 concentration of 0.083 pg m⁻³ at Little Fox Lake (Canadian sub-arctic site) and Xiao et al. (2012) (55) measured BDE-71 in the atmosphere of the Tibetan Plateau at an average concentration of 0.003 pg m⁻³.

Several Arctic studies have shown a summer maximum of the lower brominated PBDE congeners, i.e. a correlation between PBDE concentrations and ambient temperature (26, 55, 56). The transport and deposition of particle-bound PBDEs, in particular BDE-209, has mainly been associated with Arctic haze phenomena (Hermanson et al., 2010), which in Greenland mainly occurs in the period November-April. Our results show a maximum of \sum_{13} PBDE in April, mainly driven by the concentrations of BDE-47 and minimum concentrations in December and January (Figure 4.24). Regarding BDE-99, a bimodal distribution with highest concentrations in March/April and August/September is evident, but with large month-to-month variation from year to year. These results do not clearly support the temperature dependence found in other studies. The lack of temperature dependence is also verified by the lack of significant correlation between log C and 1/T.

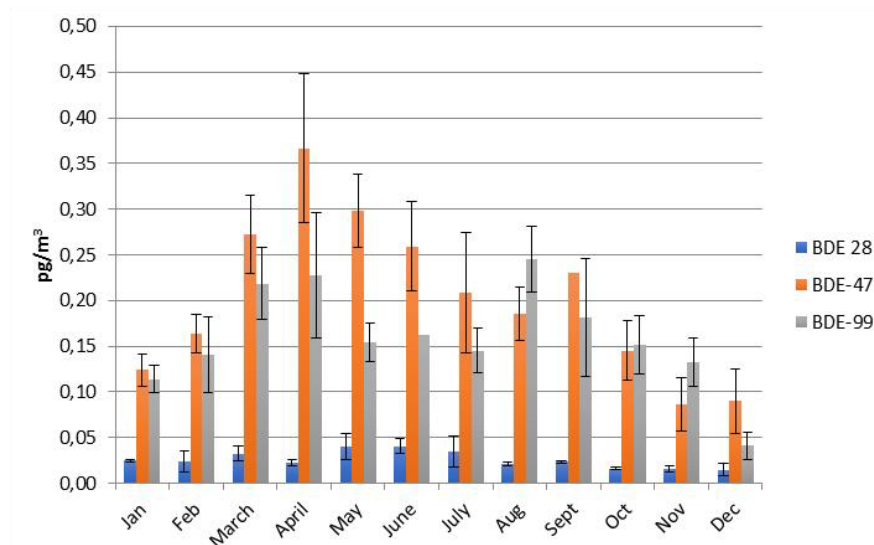


Figure 4.24. Monthly time series (average of 2008-2015) of BDE-28, BDE-47 and BDE-99 concentrations. The error bars indicate \pm standard deviation of the measurements.

Compared with PCBs, the particle-bound fraction of PBDEs in air is larger, as reflected by their higher $\log K_{OA}$ values (Harner and Shoeib, 2002) and lower vapour pressure. For temperatures of 0 °C, the authors predicted that 88 and 97 % of BDE-47 and BDE-99, respectively, would be associated with particles, in contrast to only 24 % of BDE-28. Thus, the particle-bound transport of PBDEs to the Arctic can be significant, even for congeners with only four Br atoms. For congeners with a higher degree of bromination, the particle-bound fraction rapidly converges towards 100 % (57), suggesting that transport processes are similar for these congeners including BDE-209 as well. Temporal trends were also investigated for PBDEs and neutral PFAS with the same method used for OCPs. For these groups of compounds it was impossible to identify a trend due to the high inter-annual variation and the relatively short time period of measurements.

Table 4.3. Average, median and concentration ranges (pg m^{-3}) of PBDEs (pg m^{-3}) in years 2008-2015 (sum of gaseous and particulate phase). Samples below the detection limit were assigned half of the detection limit value. The values are given only for those compounds detected in more than 30 % of the samples.

Compound	Average	Median	Range
PBDE-17	0.016	0.006	0.005-0.21
PBDE-28	0.032	0.020	0.010-0.69
PBDE-71	0.026	0.007	0.005-0.82
PBDE-99	0.16	0.10	0.03-2.19
PBDE-100	0.042	0.023	0.010-0.43
PBDE-153	0.031	0.010	0.010-0.24
PBDE-154	0.025	0.010	0.010-0.21

4.4.3 Neutral perfluoroalkylated substances (PFASs)

Atmospheric concentrations (sum of gas phase and particulate phase) of the analysed PFASs in the period 2008-2015 are summarized in Table 4.4.

Table 4.4. Average, median and concentration ranges (pg m^{-3}) of neutral PFASs (pg m^{-3}) in years 2008-2015 (sum of gaseous and particulate phase). Samples below the detection limit are assigned half of the detection limit value. The values are given only for those compounds detected in more than 30 % of the samples.

Compound	Average	Median	Range
6:2 FTOH	2.73	1.93	0.23-16.5
8:2 FTOH	4.48	3.37	0.23-22.4
10:2 FTOH	1.32	0.67	0.10-9.68
N-Me-FOSA	0.34	0.22	0.10-3.41
N-Et-FOSA	0.30	0.22	0.11-1.93
N-Me-FOSE	0.48	0.28	0.07-7.46
N-Et-FOSE	0.57	0.22	0.06-5.96

The average yearly sum of the seven measured neutral PFAS ($\Sigma_7\text{PFAS}$) in the atmosphere at VRS ranged from 1.82 to 32.1 pg m^{-3} . The most abundant compound is 8:2 FTOH (44% of $\Sigma_7\text{PFAS}$), followed by 6:2 FTOH (25% of $\Sigma_7\text{PFAS}$) and 10:2 FTOH (14% of $\Sigma_7\text{PFAS}$). Among the FOSA/FOSE, the dominant compound was N-Me-FOSE (average: 0.61 pg m^{-3}) followed by N-Et-FOSE (average: 0.50 pg m^{-3}), N-Me-FOSA (average: 0.44 pg m^{-3}) and N-Et-FOSA (0.33 pg m^{-3}). The concentrations of 6:2 FTOH measured in this study are in the same range as those reported by other Arctic studies. The concentrations of 8:2 and 10:2 FTOH are comparable with those observed at Alert (58) and at Ny Ålesund (59). 8:2 and 10:2 FTOH concentrations reported by others (60-62) are between four and ten times higher than those reported in this study. This could be explained by the fact that these results are produced during campaigns carried out in the spring/summer months, when the concentrations are relatively higher than the rest of the year at least for 8:2 FTOH.

8:2 FTOH generally contributes from 50 to 60 % to the total FTOH concentration, as observed (e.g. 61, 62). An increased proportion of 8:2 FTOH in air masses from remote areas can be explained by the longer residence time of 8:2 FTOH (~80 days) than those of 6:2 FTOH and 10:2 FTOH (50 and 70 days, respectively) (63). The average 6:2 FTOH to 8:2 FTOH to 10:2 FTOH ratio in the present study is 1.7: 3.1: 1.8, which is similar to ratios reported by other studies in the Arctic (59, 62), indicating that the FTOH concentrations measured at VRS are mainly originated by long-range transport. However, long-range transport should lead to a seasonal behaviour with maximum in late winter and spring as discussed earlier. Instead, the seasonal trends of FTOHs showed increased concentrations in the summer months. Therefore, the transport mechanism of neutral PFAS to the Arctic must be more complex. The seasonal trends are not so clear for FOSA/FOSE, due to very low concentrations of these compounds combined with high variation in the monthly concentrations during the six-years measuring period. The correlation between PFAS concentrations and ambient temperatures calculated with the CC equation is not significant. Lack of significant correlation between FTOHs concentrations and temperature is also observed at Ny Ålesund (59). Xie et al. (2015) further observed net fluxes of FTOHs from snow to the atmosphere, which indicated re-evaporation of FTOH scavenged from the atmosphere to the snow.

4.4.4 Hexabromocyclododecane (HBCDD)

HBCDD could be detected in the majority of filter samples analysed since 2012. The Σ HBCDD concentration ranged from below detection limits to 1.3 pg m^{-3} measured in September 2012. Figure 4.22 shows annual mean concentrations for the individual isomers and Σ HBCDD. As concentrations below detection limits are replaced by zero, the annual means might be slightly underestimated. The concentration of Σ HBCDD decreases in the order 2012 = 2014 < 2015 < 2013. The reasons for the low levels in 2013 are unclear. If the samples from 2013 are not blank corrected, the annual mean would be 0.15 pg m^{-3} , i.e. more similar to that of 2015.

HBCDD has been monitored at the Arctic stations Alert (Canada) and Pallas (Finland) since 2002 and 2013, respectively, but is mostly undetectable (49). At the Zeppelin monitoring station on Svalbard, Σ HBCDD decreased from 7.1 pg m^{-3} in 2006 to 0.65 pg m^{-3} in 2014 (64). However, only five samples were reported above the detection limits for either α -HBCDD or γ -HBCDD in 2014, ranging from 0.03 to 0.71 pg m^{-3} . They might indicate somewhat higher levels than those at VRS.

At the Arctic/sub-arctic stations of the Global Atmospheric Passive Sampling (GAPS) network, HBCDD was analysed at Barrow, Alaska (between not detected to 2.0 pg m^{-3}), St. Lawrence Island, Canada (at 0.22 pg m^{-3}), Stórhöfði, Iceland (between not detected to 3.3 pg m^{-3}) and Ny-Ålesund, Svalbard (between not detected to 5.1 pg m^{-3}), in samples from 2005 (65). Due to the limitations of the passive sampling technique these measurements are probably not directly comparable to those at VRS.

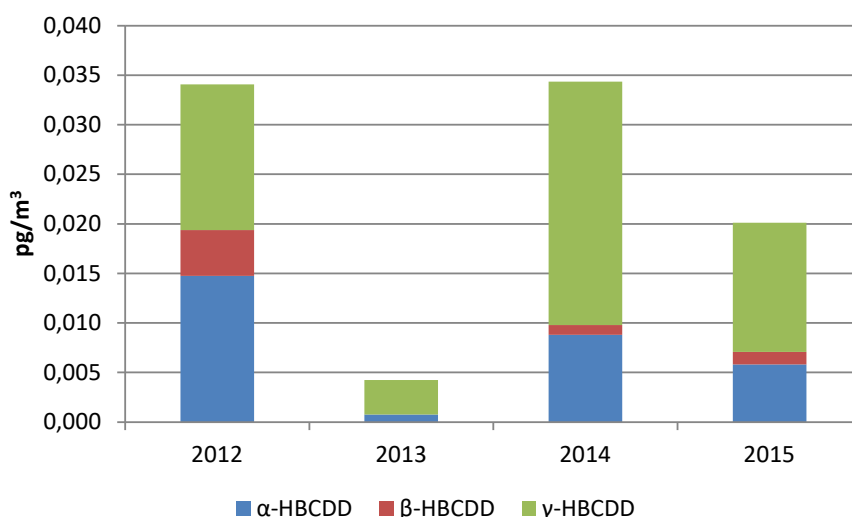


Figure 4.25. Annual mean concentrations (pg m^{-3}) of HBCDD in filter samples from Villum Research Station. N=12 in 2012, N=10 in 2013, N=12 in 2014 and N=11 in 2015. Concentrations below detection limits were replaced by zero in the mean calculations.

Figure 4.25 shows that the samples are slightly enriched in α -HBCDD compared with its percentage of 10-13 % in technical HBCDD. On average, α -HBCDD accounts for 23 % of Σ HBCDD in the particles. A conversion of γ - to α -HBCDD can take place already during polymer production or processing if temperatures exceed 160 °C (14). Similar behaviour has also been shown to

occur for HBCDD associated with light-exposed dust (66). However, compared with Arctic biota samples, some of which only contain α -HBCDD (67), the HBCDD composition in the Arctic air samples is still fairly close to the technical mixture.

The monthly resolution of the Σ HBCDD concentrations does not show any clear seasonal trend (Figure 4.26). The most recent data from 2015 indicates higher concentrations in the winter, but previous samples are not in line with this observation. Specifically, the high concentration in September 2012 as well as relatively high concentrations in July, August and September 2014 do not follow this trend. A tendency towards higher concentrations in winter was observed in the HBCDD monitoring at Zeppelin Mountain, Svalbard (64).

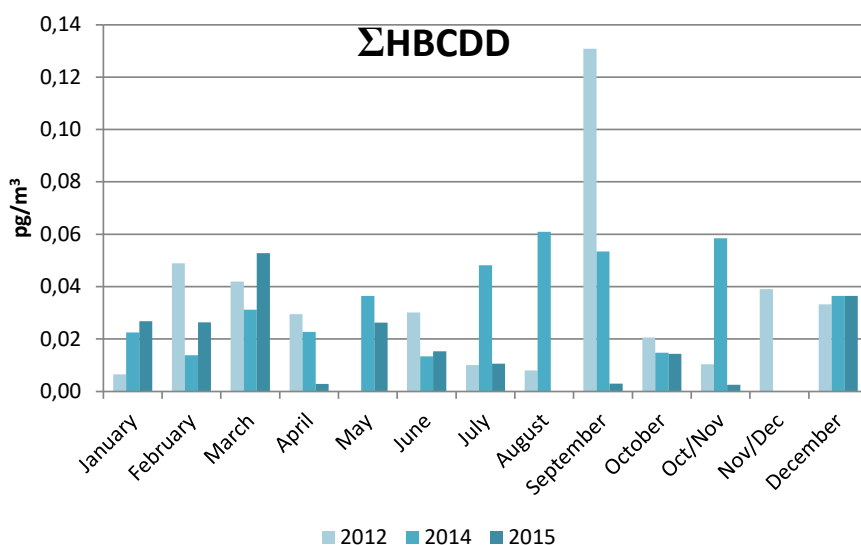


Figure 4.26. Concentration of Σ HBCDD (in pg m^{-3}) on filters from monthly air collection at Villum Research Station in 2012, 2014 and 2015. Data from 2013 are omitted because many values are below detection limits. No samples were available for the following months: May 2012, November/December 2014, August 2015 and November 2015. Concentrations below detection limits were replaced with zero in the calculation of Σ HBCDD.

In summary, the four time series is too short to provide time trend, but given the recent regulations of HBCDD and observations of decreasing concentrations in other time series, it will be relevant to continue monitoring HBCDD in Greenland air. The HBCDD concentrations are low, but detectable, and slightly lower than at Svalbard, which could be explained by a latitudinal decrease. The HBCDD composition is similar to the technical mixture, albeit slightly enriched in α -HBCDD, and thus clearly different from the HBCDD composition in Arctic wildlife. No clear seasonal trend can be established yet.

4.4.5 Comparison of modelled and measured α -HCH

α -HCH is the major component of technical HCH, one of the most applied organochlorine insecticides worldwide (68), see section 4.3.1. The use of technical HCH is banned in several countries in the late 1970s and onwards, and in 2009 it is added to the Stockholm convention on POPs. Residues from previous year's usage are still evaporating from source regions due to the long lifetime in soil and the large amounts applied.

The use of a sandwich of PUF-XAD-PUF at VRS in the measurements of e.g. α -HCH makes the data set unique. Other stations use only PUF and thus have large blank trough and cannot collect α -HCH quantitatively.

Modelled α -HCH concentrations

Measured α -HCH data is compared with results from a simulation with the DEHM model covering the period from 1989 to 2015. DEHM is run using meteorological data from the MM5 meteorological model as driver. The emission estimates are based on the estimates from (32, 69) up until 2000. The emissions from 2000 and onwards are estimated to be exponentially decreasing with an e-fold time of 10 years. To account for α -HCH deposited from usage in the years prior to 1989 an initial field in ocean water based on measurements (69) and an initial field in soil based on a long-term spin-up simulation (32) is applied.

There is a clear seasonal signal in the simulated concentrations with highest concentrations in summer and lowest in winter (Figure 4.27). The simulated summer concentrations are higher or at the same level as the measured concentrations, while the simulated concentrations in autumn, winter and spring are lower than the measured concentrations.

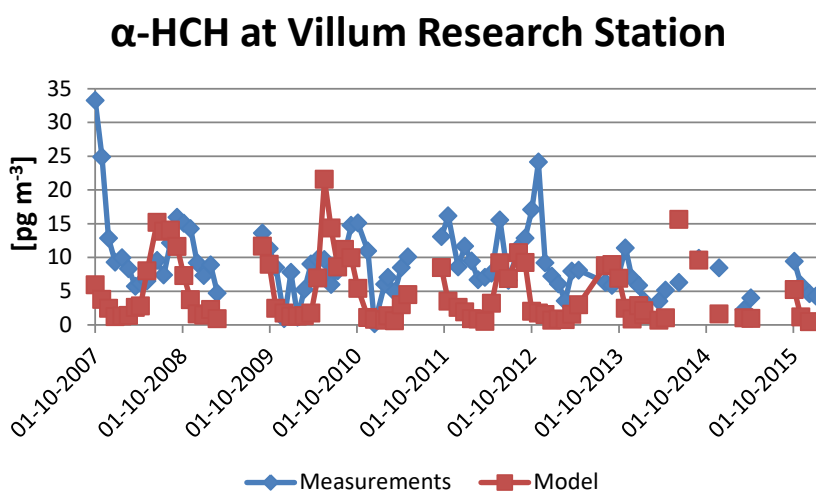


Figure 4.27. Measured (\diamond) and simulated (\square) α -HCH concentrations in pg m^{-3} at VRS.

The atmospheric transport to the Arctic is low due to no or very low primary emissions in source areas. The major source to atmospheric α -HCH concentrations in the Arctic is thus expected to be re-volatilization from the surface, especially from the ocean where large amounts of α -HCH has accumulated over the past decades. The half-life in Arctic Ocean water is in the order of 10-20 years (70). The observed concentrations supports that reemission from the ocean is the primary source to the α -HCH concentrations. The measurements peak in late summer and early autumn, where the sea surface temperature is at its maximum, and the sea ice coverage is at its minimum, thus offering the optimal conditions for re-volatilization. This seasonal pattern is not well captured by the model. The reason for this is that the ocean compartment in the model is very simple, describing only a surface layer with a fixed depth and

no horizontal movement. This description is not adequate to describe the seasonal variations in details when the primary source to atmospheric concentrations is the ocean. The model has previously performed better compared to measurements for the period before year 2000 (32, 69), where the atmospheric concentrations were dominated by primary emissions. This illustrates the challenges we face describing the environmental fate of POPs in a world that shifts from domination of primary to secondary sources (71).

4.5 Monitors (GEM and O₃)

The measurements of GEM and ozone from 1996 and onwards is seen in Figure 4.28.

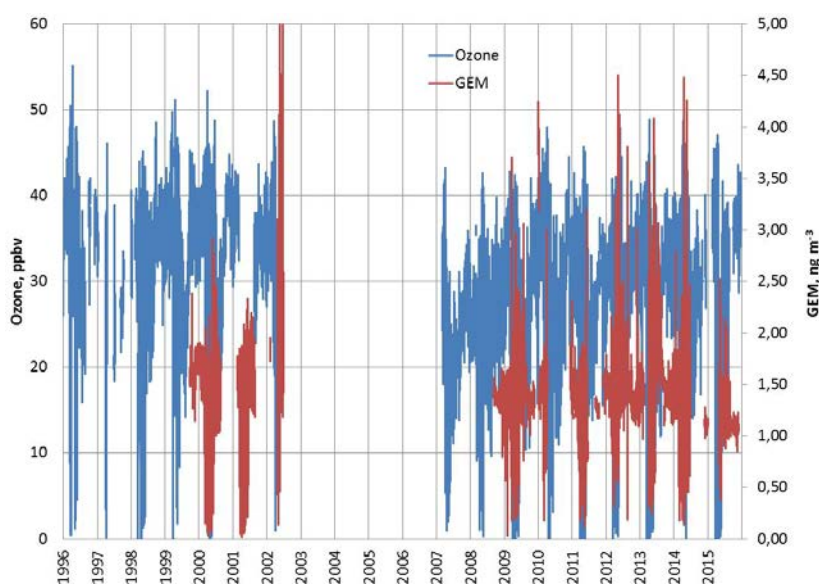


Figure 4.28. Time series of ozone and GEM at VRS from 1996 to 2015

A seasonal pattern is observed each year. In January and February, the level of ozone and GEM is rather stable. After the polar sunrise the concentration starts to fluctuate strongly and ozone and GEM are depleted fast within a few to 10 hours. The data until 2002 is used to investigate if one reactant could remove both ozone and GEM. There is indeed found such a factor and a reaction rate was extracted, (23) which fitted well with a reaction rate of Br initiated reactions determined by theoretical chemistry (72, 73). A similar study was made on the data from 2007 and onwards. A part of the period, GEM is measured with a time resolution of 1 hour and this is unfortunately too low a resolution to determine the kinetics of the reaction and this period has therefore been removed from the dataset. With the new data the same calculations are made. The same results were obtained though the uncertainty on the resulting slope was much larger due to the general lower concentration of GEM.

4.5.1 GEM trend

Table 4.5 shows the yearly average GEM concentration excluding the period with mercury depletion and periods with reemission. The periods from 15 October to 31 December are shown. The date of the first observed depletion and the date where the first reemission occurs is also evident from the table.

Table 4.5. The average concentration of GEM outside the depletion period and reemission period chosen to be between 15 October to 31 December. The day for first observed depletion is defined as 15 % of the average winter GEM concentration and reemission is defined to be values above 2.0 ng m⁻³.

Year	First Depletion	First Reemission	Average, event free [GEM] (ng m ⁻³)
2000	5/3	25/5	1.66
2001	17/2	n.a.*	1.64
2008	9/3	n.a.	1.37
2009	9/1	21/3	1.36
2010	18/2	6/4	1.47
2011	1/3	7/6	1.28
2012	3/2	10/4	1.27
2013	16/1	<15/4	1.42
2014	17/2	14/3	1.12
2015	n.a.	n.a.	1.09

*n.a. = none analysis

There is a significant trend in the concentration of GEM as seen in Figure 4.29. There is a decrease of GEM of 0.03 ng m⁻³ year⁻¹ (significant on a 99.9 % confidence interval). This decrease is independent of the 2 first years, so without 2000 and 2001 the decrease is unchanged.

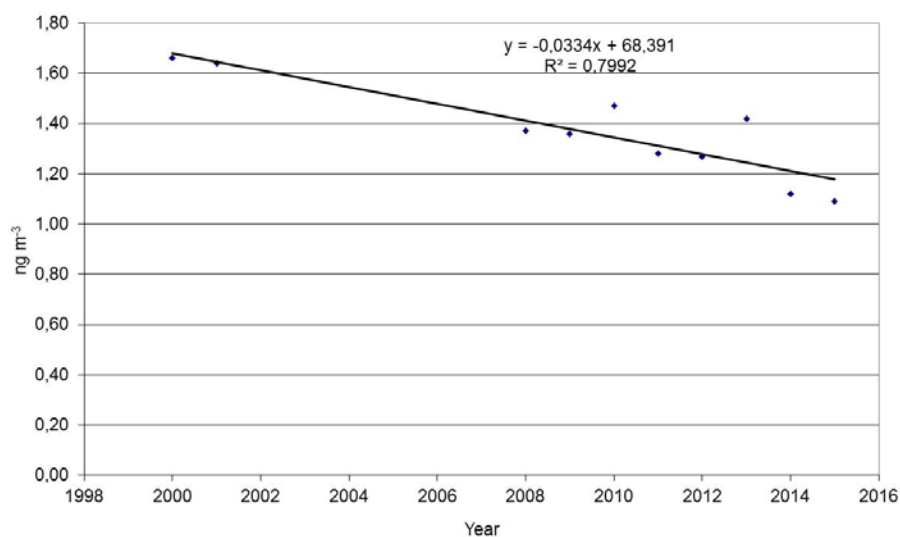


Figure 4.29. The trend line for the average concentrations of GEM during the non-depletion period shown in Table 4.5.

There is no significant trend in the period of neither the arrival of the first depletion nor the start of the reemission (not even at a confidence level as low as 80%). This is interesting as the fate of GEM is believed to depend on the presence of seasonal sea ice, solar radiation and the presence of air temperatures below $-4\text{ }^{\circ}\text{C}$. See Figure 4.30 for a conceptual description of mercury removal.

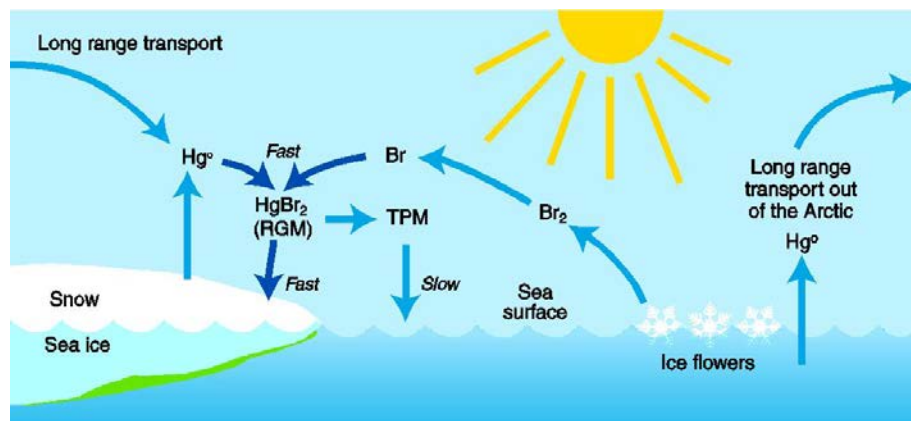


Figure 4.30. The mercury cycle in the Arctic atmosphere where elemental mercury (Hg^0) is converted to reactive gaseous mercury (RGM) that either is fast removed or converted into total particulate mercury (TPM).

In the previous 10 years the emission of mercury is considered to be relatively constant (74, 75) though the geographical distribution in the emissions has changed from the heavy industrial areas in East USA and Europe to China. Thus the trend has to be explained by the transport pattern to Arctic and by the removal processes of atmospheric mercury. This is subject to on-going work.

4.5.2 Ozone trends

Ozone concentrations are also analysed for possible trends. In figure 4.31 the average ozone concentration is presented excluding the depletion period from March to end of May. There is a significant decrease over the 20-year period of $0.3\text{ ppbv year}^{-1}$ on a 95 % confidence interval. This decrease is entirely due to the difference between the first years (1996-2000) and the second period (2007-2015). There is no trend in the period 1996 to 2000 or from 2007 to 2015. As the data is not continuous due to the interruption of measurements and thus lack of data from 2001 to end of 2006 caution is needed when looking at the entire period.

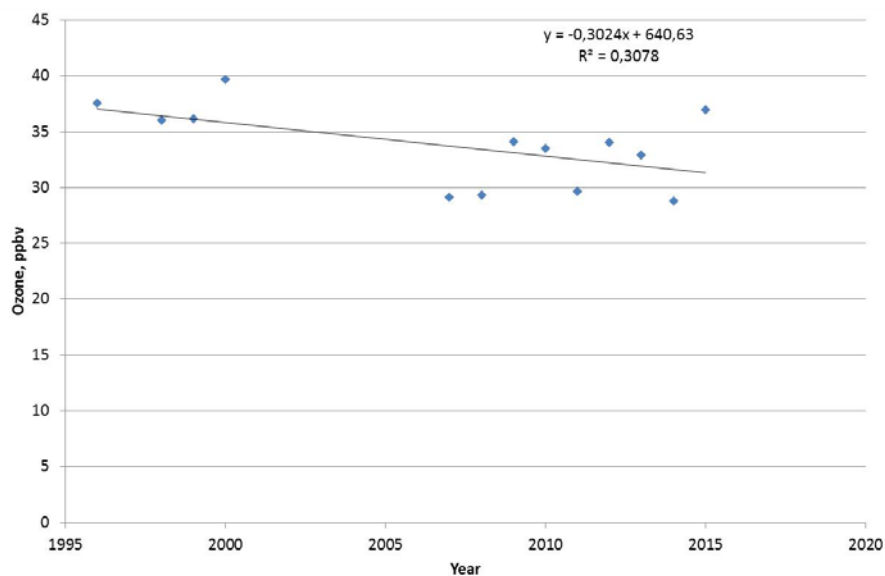


Figure 4.31. The trend line for the average concentrations of ozone during the non-depletion period shown in Table 4.5.

More data is needed in order to say something definitive on ozone trend especially as we at present have no explanation for the observation.

4.6 PFAS in snow

Samples for analysis of PFAS are collected in the snowpack around the station, which is only influenced by precipitation. Thus, the presence of the acidic PFAS in snow only originates from atmospheric deposition and oxidation of the neutral precursors measured in the atmosphere (4.3.3).

The compounds found with detection frequencies over 50 % were perfluorocarboxylates (PFCAs) with carbon atoms number between 6 and 11 (PFHxA, PFHpA, PFOA, PFNA, PFDA and PFUnA) and PFOS. PFDoA was found in 33 % of the samples, while the PFCAs with longer chain and the other perfluorosulfonates were never detected. The highest average concentrations ranged from 0.46 to 0.06 ng/L, in the order PFNA>PFOA>PFHpA>PFOS>PFDA>PFUnA>PFHxA>PFDoA. The composition of PFCAs in snow reflects the composition of precursor compounds (FTOH) measured in the atmosphere. Since 8:10 FTOH was the precursor measured at highest atmospheric concentrations and the corresponding oxidised compound (PFNA) has the highest concentrations in snow samples. PFOS was also detected at relatively high concentrations; however, the precursor compounds of PFOS (methyl and ethyl-perfluorosulfonamides and perfluorosulfonamidoethanols) were detected at much lower concentrations than the FTOHs. Thus, the origin of PFOS deposition is still uncertain and the presence of other possible precursors (e.g. PFOSA) should be investigated in the atmosphere.

Table 4.6. Average, median and concentration ranges (ng L⁻¹) of PFASs detected in snow (2008-2015).

Compound	Average	Median	Range	Detection frequency (%)
PFOS	0.31	0.33	0.02-0.73	52
PFHxA	0.12	0.13	0.08-0.15	93
PFHpA	0.33	0.31	0.11-1.46	93
PFOA	0.42	0.24	0.09-0.82	86
PFNA	0.46	0.12	0.06-1.88	69
PFDA	0.13	0.07	0.01-0.51	67
PFUnA	0.13	0.05	0.01-0.47	55
PFDoA	0.06	0.04	0.01-0.17	33

PFAS concentrations found at VRS are similar to those found in Northern Sweden (76) and Svalbard (59), where PFAS concentrations were in the range 0.07 to 0.34 ng/L and 0.33 to 0.69 ng/L, respectively. A study of snow collected in 2008 from the Devon Ice cap in the Canadian Arctic (a follow-up to the original study by (77)) also reported similar concentrations for PFOA (0.07-0.68 ng/L), 0.030–1.42 ng/L for PFNA, and 0.01–0.23 ng/L for PFDA to those at VRS (DeSilva and Muir, private communication 2016).

4.7 Mercury in snow

In Table 4.7 is shown the concentration of mercury in surface snow from VRS. As the data for mercury is very sparse data from the first half year of 2016 are included here.

Table 4.7. The concentration of mercury in surface snow in ng L⁻¹.

Date	Concentration	Identification
01-03-2012		125
01-03-2012		130
01-03-2012	0.73	110
01-03-2012	0.90	107
15-03-2012	1.54	112
15-03-2012		113
01-05-2014	0.60	2014-13651 Hg
02-05-2014	0.68	2014-13652 Hg
01-12-2014	0.49	P1
01-12-2014	0.51	P2
01-12-2014	0.48	P3
14-12-2015		ATRO-2016-14954
04-01-2016		ATRO-2016-14955
01-02-2016		ATRO-2016-14956
01-03-2016		ATRO-2016-14957
01-04-2016		ATRO-2016-14958
25-04-2016	8.8	123
26-04-2016	1.1	129
01-05-2016	6.2	113
	0.3	115

Most of the samples are within a range comparable with Danish concentrations in rainwater (close to 1 ng L⁻¹). Even during mercury Depletion events we have not observed any elevation of mercury in snow until spring 2016.

During spring 2016 the surface snow concentrations were much more variable with a max concentration 25 April of 8.8 ng L⁻¹ after which followed a low value of 1.1 ng L⁻¹ again. Though this is more than 10 times higher than otherwise measured this level is much lower compared to reported levels elsewhere in High Arctic (e.g. at Point Barrow, Alaska (78), where levels up to 132 ng L⁻¹ has been reported). An important question is; how much of the mercury is bio-available and we have previously shown that a significant part is available for bacteria and algae (79).

The snow sampling at VRS has been intensified throughout 2016 and 2017 and it will be very interesting to see the coming results.

5 Conclusion and recommendations

This report describes the results obtained in the Danish contribution to the Arctic Monitoring and Assessment Program (AMAP), the atmospheric part. The longest data series goes back to 1990 but many are from 2008. This forms a strong base for evaluating trends, yearly differences and seasonal patterns. We are using the integrated monitoring strategy, where measurements and models are performed in order to obtain most information from the funded activities. Focus is on process understanding in order to evaluate the consequences of abatement and legislative initiatives and potentially enable optimization of these. Some of the main findings and conclusions from this report are highlighted below.

5.1 SO_x

The main source of sulphur dioxide and sulphate at VRS are anthropogenic emission at mid latitudes. The main reasons for observations of changed pollution levels in the Arctic atmosphere are still the change of anthropogenic emission for most species. In future, we expect that the change in transport pathways due to a still faster climatic change will play a more significant role than observed hitherto.

The concentrations of sulphur dioxide and sulphate are still interesting though the levels have been continuously decreasing. They demonstrate that the DEHM describes the transport of anthropogenic emitted species at mid-latitudes very well. Looking more into details there is still discrepancies in the description of these species. The discrepancies are due to the uncertainty in emission inventories of anthropogenic emission of mainly sulphur dioxide.

The concentrations of SO_x are modelled for a 36-year period using the DEHM model. The levels decrease over the period following a general decrease in emissions from mid-latitude source areas. Larger decreases are seen for VRS and Svalbard than for other Arctic sites that are due to the proximity of European sources that are reduced mostly. In agreement with this, we observe a significant decreasing trend of both sulphur dioxide and sulphate from 1990 to 2015. Furthermore, there is a strong seasonal variation where sulphur dioxide builds up during winter and peaks in January. Thereafter sulphur dioxide decreases, and sulphate starts to build and reaches a broader maximum in end of March to the beginning of May. The appearance of this seasonal behaviour is explained by the position of the polar front over the year, the variation in source strength and by the appearance of polar sunrise in the end of February. With the polar sunrise, photochemical processes start oxidizing sulphur dioxide to sulphate and the solar heat creates more turbulence in the atmosphere leading to faster deposition of pollutants.

5.2 Other inorganic species

Other inorganic compounds show different seasonal behaviour and trends, which is explained by considering their sources, transport pattern and removal processes. For example Al and Fe have soil as a main sources and their appearance are closely connected to windblown dust.

Pb is found to have the same seasonal behaviour as sulphate and it shows a significant decrease from 1990 to 2015. This fits well with the decreasing Pb emission that is explained by the fact that Pb is now used as additive in gasoline and due to development of modern engine technology in vehicles as well as exhaust treatment.

The comparison of modelled and measured concentrations of Pb show a measured/modelled ratio of 1.28 in 1990-1993 and 0.42 in 2012-2014. The ratio has decreased with a factor of about 3 due to reductions in Pb emissions in the source regions in Eurasia, which the model is not taking into account.

5.3 Persistent Organic Pollutants

A long series of POPs have been measured since 2008. Though the time series is relatively short, significant trends have been observed for many of the compounds. The reasons behind observed trends are at the moment only speculative as emission inventories are not available. An exception is α -HCH and detailed studies have been made, where model results have been validated by comparison to measurements, and based on this new parameterisation has been developed.

The DEHM model tends to underestimate the measured concentrations of α -HCH, although the maximum levels are well captured. The predicted seasonal pattern is not following the measured seasonal pattern well. This is probably due to the simple description of the surface ocean compartment in the model, which in the present regime is dominated by secondary sources that are not sufficiently detailed to capture the dynamics. These parameters are very important for describing α -HCH because the anthropogenic emissions in the main source region has ceased and the release from e.g. surface water is getting more important. From our study, it is evident that we need a better description of inter-compartment transport for α -HCH, but also for all other compounds, where transport between matrixes is important. The final fate of POPs is very dependent on this transport and can in the end lead to underestimation of the time, where we need to consider a compound being mobile and thus an environmental problem or hazard.

5.4 Mercury and ozone

The dynamics of mercury and ozone have been confirmed to be closely related during Polar Spring, which most likely can be explained by mutual dependence on the release of bromine from sea areas creating mercury depletion episodes (MDE) and ozone depletion episodes (ODE). We have looked into the trend of appearance and duration of MDE and ODE, but so far no particular feature or trend has been observed.

5.4.1 Mercury

The measurements of GEM have been carried out since 1999. The yearly statistics the first years are compromised by the fact that measurements were only performed half-yearly. From 2007 yearly measurements have been carried out and from 2015 two instruments have been measuring in parallel to ensure the data coverage. This changes the statistical weight when making trend studies. Nevertheless, measurements show a decreasing trend during autumn of $0.03 \text{ ng m}^{-3} \text{ year}^{-1}$, whereas no trend in the appearance or change in the arrival and end of mercury depletion episodes can be observed. The decreasing trend in autumn can be explained by changes in transport pattern to the Arctic and by changes in removal processes. Changes in source regions might also be an important - if not the most important - reason for the observation.

5.4.2 Ozone

The depletion of ozone is following the one for GEM and thus there is not any trend in the appearance and duration of ODE. There is no trend for the ozone concentration in autumn in the two periods from 1996 to 2000 and from 2007 to 2015. A trend is observed when looking at the entire period together, where ozone is decreasing $0.3 \text{ ppb year}^{-1}$. Due to the interruption of the data series large caution has to be taken and more data will be needed. Furthermore, there is at present no ab initio model that can describe ODE in Polar Regions troposphere. More focus will be on ozone in the future due to its central role for understanding atmospheric photochemistry, its role as pollutant and its role as a climate forcer.

5.5 Snow samples

5.5.1 PFAS

PFAS has been measured in surface snow in the period from 2008 and 2015. The concentrations found are comparable to those found at other high Arctic sites. The presence of perfluorocarboxylates (PFCAs) with carbon atoms number between 6 and 11 is in agreement with that the origin of deposition is from the oxidation of the neutral precursors (FTOH) detected in the atmosphere.

5.5.2 Mercury

In general, the measured mercury concentrations at VRS are low. In spring 2016 higher levels of mercury was observed though they were still a factor of 10 lower than e.g. found at Point Barrow in Alaska.

More frequent samples have been collected in 2016 and 2017 and hopefully these values will reveal how important surface mercury is. An important issue is that the quantitative understanding of the fluxes between matrixes (atmosphere/ice/snow surfaces/sea water/biota).

6 Acknowledgement

“The Danish Environmental Protection Agency” financially supported this work with means from the MIKA/DANCEA funds for Environmental Support to the Arctic Region. The Royal Danish Air Force is acknowledged for providing free transport to Station Nord, and the staff at Station Nord is especially acknowledged for excellent support. Villum Foundation is acknowledged for the large grant making it possible to build the new research station, Villum Research Station (VRS), Station Nord.

The Technicians in Department of Environmental Science, Aarhus University are acknowledged for excellent work analysing the collected samples. Christel Christoffersen and Bjarne Jensen are specially acknowledged for being key technicians in the project and for excellent technical work at Villum Research Station.

7 References

1. IPCC. IPCC Fifth assessment report. 2013 2013.
2. Stendel M, Christensen JH, Petersen D. Arctic climate and climate change with a focus on Greenland. In: Meltofte H, Christensen TR, Elberling B, Forchhammer MC, Rasch M, editors. *Advances in Ecological Research, Vol 40: High-Arctic Ecosystem Dynamics in a Changing Climate*. *Advances in Ecological Research*. 40. San Diego: Elsevier Academic Press Inc; 2008. p. 13-43.
3. Bossi R, Skjoth CA, Skov H. Three years (2008-2010) of measurements of atmospheric concentrations of organochlorine pesticides (OCPs) at Station Nord, North-East Greenland. *Environmental Science-Processes & Impacts*. 2013;15(12):2213-9.
4. Christensen JH, Brandt J, Frohn LM, Skov H. Modelling of mercury in the Arctic with the Danish Eulerian Hemispheric Model. *Atmos Chem Phys*. 2004;4:2251-7.
5. Ferrari CP, Dommergue A, Boutron CF, Skov H, Goodsite M, Jensen B. Nighttime production of elemental gaseous mercury in interstitial air of snow at Station Nord, Greenland. *Atmospheric Environment*. 2004;38(17):2727-35.
6. Goodsite M, Skov H, Asmund G, Bennike O, Feilberg A, Glasius M, et al. Pilot Study of Contaminants near Station Nord, a Military Airbase and Research Station in NE Greenland. *NATO Advanced Research Workshop on Sustainable Cities and Military Installations: Climate Change Impact on Energy and Environmental Security Proceedings*. 2014:177-98.
7. Heidam NZ, Christensen J, Wåhlin P, Skov H. Arctic atmospheric contaminants in NE Greenland: levels, variations, origins, transport, transformations and trends 1990-2001. *Science of the Total Environment*. 2004;331(1-3):5-28.
8. Hung H, Kallenborn R, Breivik K, Su YS, Brorstrom-Lunden E, Olafsdottir K, et al. Atmospheric monitoring of organic pollutants in the Arctic under the Arctic Monitoring and Assessment Programme (AMAP): 1993-2006. *Science of the Total Environment*. 2010;408(15):2854-73.
9. Nguyen QT, Kristensen TB, Hansen AMK, Skov H, Bossi R, Massling A, et al. Characterization of humic-like substances in Arctic aerosols. *Journal of Geophysical Research-Atmospheres*. 2014;119(8):5011-27.
10. Nguyen QT, Skov H, Sorensen LL, Jensen BJ, Grube AG, Massling A, et al. Source apportionment of particles at Station Nord, North East Greenland during 2008-2010 using COPREM and PMF analysis. *Atmos Chem Phys*. 2013;13(1):35-49.
11. Skov H, Christensen J, Asmund G, Rysgaard S, Nielsen TG, Dietz R, et al. Fate of mercury in the Arctic (FOMA). *NERI Technical Report; 2004* 2004. Report No.: 511.
12. Hoh E, Hites RA. Brominated flame retardants in the atmosphere of the east-central United States. *Environ Sci Technol*. 2005;39(20):7794-802.

13. de Wit CA, Herzke D, Vorkamp K. Brominated flame retardants in the Arctic environment - trends and new candidates. *Science of the Total Environment*. 2010;408(15):2885-918.
14. Covaci A, Gerecke AC, Law RJ, Voorspoels S, Kohler M, Heeb NV, et al. Hexabromocyclododecanes (HBCDs) in the environment and humans: A review. *Environ Sci Technol*. 2006;40(12):3679-88.
15. ECHA. Inclusion of substances of very high concern in the candidate list (Decision by the Executive Director). Helsinki, Finland: European Chemicals Agency Document ED/67/2008. ; 2008.
16. EU. Directive 2013/39/EU of the European Parliament and of the Council of 12 August 2013 amending Directives 2000/60/EC and 2008/105/EC as regards priority substances in the field of water policy. . In: 226/1. OJotEUL, editor. 2013.
17. OSPAR. OSPAR Background Document on certain brominated flame retardants. . In: Series. HS, editor. 2009.
18. UNECE. Options for revising the protocol on persistent organic pollutants. Report by the Co-Chairs of the Task Force on Persistent Organic Pollutants. Executive Body for the Convention on Long-Range Transboundary Air Pollution.: United Nations Economic Commission for Europe, Geneva, Switzerland.; 2009.
19. UNEP. Listing of hexabromocyclododecane.; 2013.
20. Sanei H, Outridge PM, Goodarzi F, Wang F, Armstrong D, Warren K, et al. Wet deposition mercury fluxes in the Canadian sub-Arctic and southern Alberta, measured using an automated precipitation collector adapted to cold regions. *Atmospheric Environment*. 2010;44(13):1672-81.
21. Christensen JH. The Danish Eulerian hemispheric model - A three-dimensional air pollution model used for the Arctic. *Atmospheric Environment*. 1997;31(24):4169-91.
22. Brandt J, Silver JD, Frohn LM, Geels C, Gross A, Hansen AB, et al. An integrated model study for Europe and North America using the Danish Eulerian Hemispheric Model with focus on intercontinental transport of air pollution. *Atmospheric Environment*. 2012;53:156-76.
23. Skov H, Christensen JH, Goodsite ME, Heidam NZ, Jensen B, Wählén P, et al. Fate of elemental mercury in the arctic during atmospheric mercury depletion episodes and the load of atmospheric mercury to the arctic. *Environ Sci Technol*. 2004;38(8):2373-82.
24. Hansen KM, Halsall CJ, Christensen JH. A dynamic model to study the exchange of gas-phase POPs between air and a seasonal snowpack. *Environ Sci Technol*. 2006;40(8):2644-52.
25. Krogseth IS, Kierkegaard A, McLachlan MS, Breivik K, Hansen KM, Schlabach M. Occurrence and Seasonality of Cyclic Volatile Methyl Siloxanes in Arctic Air. *Environ Sci Technol*. 2013;47(1):502-9.
26. Bossi R, Skov H, Vorkamp K, Christensen J, Rastogi SC, Egelov A, et al. Atmospheric concentrations of organochlorine pesticides, polybrominated diphenyl ethers and polychloronaphthalenes in Nuuk, South-West Greenland. *Atmospheric Environment*. 2008;42(31):7293-303.

27. Lamarque JF, Bond TC, Eyring V, Granier C, Heil A, Klimont Z, et al. Historical (1850-2000) gridded anthropogenic and biomass burning emissions of reactive gases and aerosols: methodology and application. *Atmos Chem Phys*. 2010;10(15):7017-39.
28. Kaiser JW, Heil A, Andreae MO, Benedetti A, Chubarova N, Jones L, et al. Biomass burning emissions estimated with a global fire assimilation system based on observed fire radiative power. *Biogeosciences*. 2012;9(1):527-54.
29. Schultz MG, Heil A, Hoelzemann JJ, Spessa A, Thonicke K, Goldammer JG, et al. Global wildland fire emissions from 1960 to 2000. *Global Biogeochemical Cycles*. 2008;22(2):17.
30. Zare A, Christensen JH, Irannejad P, Brandt J. Evaluation of two isoprene emission models for use in a long-range air pollution model. *Atmos Chem Phys*. 2012;12(16):7399-412.
31. Guenther A, Karl T, Harley P, Wiedinmyer C, Palmer PI, Geron C. Estimates of global terrestrial isoprene emissions using MEGAN (Model of Emissions of Gases and Aerosols from Nature). *Atmos Chem Phys*. 2006;6:3181-210.
32. Hansen KM, Halsall CJ, Christensen JH, Brandt J, Frohn LM, Geels C, et al. The role of the snowpack on the fate of alpha-HCH in an atmospheric chemistry-transport model. *Environ Sci Technol*. 2008;42(8):2943-8.
33. Breivik K, Sweetman A, Pacyna JM, Jones KC. Towards a global historical emission inventory for selected PCB congeners - A mass balance approach-3. An update. *Science of the Total Environment*. 2007;377(2-3):296-307.
34. Wilson SM, J.; Sundseth, K.; Kindbom, K.; Maxson, P.; Pacyna, J.; Steenhuisen, F. Updating Historical Global Inventories of Anthropogenic Mercury Emissions to Air. Oslo, Norway: Arctic Monitoring and Assessment Programme (AMAP); 2010.
35. Pacyna JM, Trevor MT, Scholtz M, Li Y-F. Global Budgets of Trace Metal Sources. *Environmental Reviews*. 1995;3:145-59.
36. Grell GA, Dudhia J, Stauffer DR. A Description of the Fifth-Generation Penn State/NCAR Mesoscale Model (MM5). Mesoscale and Microscale Meteorology Division. National Center for Atmospheric Research. Boulder, Colorado,; 1995 1995.
37. Skamarock WCK, J. B.; Dudhia, J.; Gill, D. O.; Barker, D. M.; Wang, W.; Powers, J. G. A description of the Advanced Research WRF Version 2. 2005.
38. Heidam NZ, Wählin P, Christensen JH. Tropospheric gases and aerosols in northeast Greenland. *Journal of the Atmospheric Sciences*. 1999;56(2):261-78.
39. Grube AG. Particulate air pollution and its characteristic sources in the high Arctic at Station Nord, N.E. Greenland. Master thesis, University of Science, University of Copenhagen. 2011 2011.
40. Doherty SJW, S. G.; Grenfell, T. C.; Clarke, A. D.; Brandt, R. E. . Light-absorbing impurities in arctic snow. *Atmos Chem Phys*. 2010;10(23).

41. Randles CR, LM; Ramaswamy, V Hygroscopic and optical properties of organic sea salt aerosol and consequences for climate forcing. *Geophysical Research Letters*. 2004;31(16).
42. Fenger M, Sorensen LL, Kristensen K, Jensen B, Nguyen QT, Nojgaard JK, et al. Sources of anions in aerosols in northeast Greenland during late winter. *Atmos Chem Phys*. 2013;13(3):1569-78.
43. Bossi R, Vorkamp K, Skov H. Concentrations of organochlorine pesticides, polybrominated diphenyl ethers and perfluorinated compounds in the atmosphere of North Greenland. *Environmental Pollution*. 2016;217:4-10.
44. Su Y, Hung H, Sverko E, Fellin P, Li H. Multi-year measurements of polybrominated diphenyl ethers (PBDEs) in the Arctic atmosphere. *Atmospheric Environment*. 2007;41(38):8725-35.
45. Halsall CJ, Gevao B, Howsam M, Lee RGM, Ockenden WA, Jones KC. Temperature dependence of PCBs in the UK atmosphere. *Atmospheric Environment*. 1999;33(4):541-52.
46. Wania F, Haugen JE, Lei YD, Mackay D. Temperature dependence of atmospheric concentrations of semivolatile organic compounds. *Environ Sci Technol*. 1998;32(8):1013-21.
47. Shunthirasingham C, Gawor A, Hung H, Brice KA, Su K, Alexandrou N, et al. Atmospheric concentrations and loadings of organochlorine pesticides and polychlorinated biphenyls in the Canadian Great Lakes Basin (GLB): Spatial and temporal analysis (1992-2012). *Environmental Pollution*. 2016;217:124-33.
48. Qu CK, Xing XL, Albanese S, Doherty A, Huang HF, Lima A, et al. Spatial and seasonal variations of atmospheric organochlorine pesticides along the plain-mountain transect in central China: Regional source vs. long-range transport and air-soil exchange. *Atmospheric Environment*. 2015;122:31-40.
49. Hung H, Katsoyiannis AA, Brorstrom-Lunden E, Olafsdottir K, Aas W, Breivik K, et al. Temporal trends of Persistent Organic Pollutants (POPs) in arctic air: 20 years of monitoring under the Arctic Monitoring and Assessment Programme (AMAP). *Environmental Pollution*. 2016;217:52-61.
50. La Guardia MJ, Hale RC, Harvey E. Detailed polybrominated diphenyl ether (PBDE) congener composition of the widely used penta-, octa-, and deca-PBDE technical flame-retardant mixtures. *Environ Sci Technol*. 2006;40(20):6247-54.
51. Birgul A, Katsoyiannis A, Gioia R, Crosse J, Earnshaw M, Ratola N, et al. Atmospheric polybrominated diphenyl ethers (PBDEs) in the United Kingdom. *Environmental Pollution*. 2012;169:105-11.
52. Bossi R, Riget FF, Dietz R. Temporal and spatial trends of perfluorinated compounds in ringed seal (*Phoca hispida*) from Greenland. *Environ Sci Technol*. 2005;39(19):7416-22.
53. Moller A, Xie ZY, Sturm R, Ebinghaus R. Polybrominated diphenyl ethers (PBDEs) and alternative brominated flame retardants in air and seawater of the European Arctic. *Environmental Pollution*. 2011;159(6):1577-83.

54. Yu Y, Hung H, Alexandrou N, Roach P, Nordin K. Multiyear Measurements of Flame Retardants and Organochlorine Pesticides in Air in Canada's Western Sub-Arctic. *Environ Sci Technol.* 2015;49(14):8623-30.
55. Xiao H, Shen L, Su YS, Barresi E, DeJong M, Hung HL, et al. Atmospheric concentrations of halogenated flame retardants at two remote locations: The Canadian High Arctic and the Tibetan Plateau. *Environmental Pollution.* 2012;161:154-61.
56. Aas WB, K., Heavy metals and POP measurements. EMEP/CCC-Report 4/2013; 2013.
57. Harner T, Shoeib M. Measurements of octanol-air partition coefficients (K_{OA}) for polybrominated diphenyl ethers (PBDEs): Predicting partitioning in the environment. *Journal of Chemical and Engineering Data.* 2002;47(2):228-32.
58. Genualdi S, Lee SC, Shoeib M, Gawor A, Ahrens L, Harner T. Global Pilot Study of Legacy and Emerging Persistent Organic Pollutants using Sorbent-Impregnated Polyurethane Foam Disk Passive Air Samplers. *Environ Sci Technol.* 2010;44(14):5534-9.
59. Xie ZY, Wang Z, Mi WY, Moller A, Wolschke H, Ebinghaus R. Neutral Poly-/perfluoroalkyl Substances in Air and Snow from the Arctic. *Scientific Reports.* 2015;5:6.
60. Shoeib M, Harner T, Vlahos P. Perfluorinated chemicals in the Arctic atmosphere. *Environ Sci Technol.* 2006;40(24):7577-83.
61. Stock NL, Furdui VI, Muir DCG, Mabury SA. Perfluoroalkyl contaminants in the Canadian Arctic: Evidence of atmospheric transport and local contamination. *Environ Sci Technol.* 2007;41(10):3529-36.
62. Ahrens L, Shoeib M, Del Vento S, Codling G, Halsall C. Polyfluoroalkyl compounds in the Canadian Arctic atmosphere. *Environmental Chemistry.* 2011;8(4):399-406.
63. Piekarczyk AM, Primbs T, Field JA, Barofsky DF, Simonich S. Semivolatile fluorinated organic compounds in Asian and western U.S air masses. *Environ Sci Technol.* 2007;41(24):8248-55.
64. Bohlin-Nizzetto PA, W.; Warner, N. Monitoring of environmental contaminants in air and precipitation. Oslo, Norway: Norwegian Institute for Air Research (NILU); 2015.
65. Lee SCS, E.; Harner, T.; Pozo, K.; Schachtschneider, J.; Zaruk, D.; DeJong, M.; Barresi, E.; Narayan, J., . Retrospective analysis of "new" flame retardants in the global atmosphere under the GAPS network. *Environ Pollut.* 2016;217:62-9.
66. Harrad S, Abdallah MAE, Covaci A. Causes of variability in concentrations and diastereomer patterns of hexabromocyclododecanes in indoor dust. *Environment International.* 2009;35(3):573-9.
67. Vorkamp K, Riget FF, Bossi R, Dietz R. Temporal Trends of Hexabromocyclododecane, Polybrominated Diphenyl Ethers and Polychlorinated Biphenyls in Ringed Seals from East Greenland. *Environ Sci Technol.* 2011;45(4):1243-9.

68. Li YF, Scholtz MT, van Heyst BJ. Global gridded emission inventories of alpha-hexachlorocyclohexane. *Journal of Geophysical Research-Atmospheres*. 2000;105(D5):6621-32.
69. Hansen KM, Christensen JH, Brandt J, Frohn LM, Geels C. Modelling atmospheric transport of alpha-hexachlorocyclohexane in the Northern Hemisphere with a 3-D dynamical model: DEHM-POP. *Atmos Chem Phys*. 2004;4:1125-37.
70. Harner T, Kylin H, Bidleman TF, Strachan WMJ. Removal of alpha- and gamma-hexachlorocyclohexane and enantiomers of alpha-hexachlorocyclohexane in the eastern Arctic Ocean. *Environ Sci Technol*. 1999;33(8):1157-64.
71. Nizzetto L, Macleod M, Borga K, Cabrerizo A, Dachs J, Di Guardo A, et al. Past, Present, and Future Controls on Levels of Persistent Organic Pollutants in the Global Environment. *Environ Sci Technol*. 2010;44(17):6526-31.
72. Goodsite ME, Plane JMC, Skov H. A theoretical study of the oxidation of Hg⁰ to HgBr₂ in the troposphere. *Environ Sci Technol*. 2004;38(6):1772-6.
73. Goodsite M, Plane J, Skov H. A Theoretical Study of the Oxidation of Hg⁰ to HgBr₂ in the Troposphere (vol 38, pg 1772, 2004). *Environ Sci Technol*. 2012;46(9):5262-.
74. Pacyna JM, Munthe J, Wilson J, Maxson P, Sundseth K, Pacyna EG, et al. Part A. Global emissions of mercury to the Atmosphere, Technical Background Report to the Global Atmospheric Mercury Assessment. 2008 2008.
75. UNEP. Global Mercury Assessment 2013: Sources, Emissions, Releases and Environmental Transport. UNEP Chemicals Branch, Geneva, Switzerland; 2013.
76. Codling G, Halsall C, Ahrens L, Del Vento S, Wiberg K, Bergknut M, et al. The fate of per- and polyfluoroalkyl substances within a melting snowpack of a boreal forest. *Environmental Pollution*. 2014;191:190-8.
77. Young CJ, Furdui VI, Franklin J, Koerner RM, Muir DCG, Mabury SA. Perfluorinated acids in arctic snow: New evidence for atmospheric formation. *Environ Sci Technol*. 2007;41(10):3455-61.
78. Brooks S, Saiz-Lopez A, Skov H, Lindberg S, Plane JMC, Goodsite ME. The mass balance of mercury in the springtime polar environment. *Geophysical Research Letters*. 2006;33:L13812.
79. Moller AK, Barkay T, Abu Al-Soud W, Sorensen SJ, Skov H, Kroer N. Diversity and characterization of mercury-resistant bacteria in snow, freshwater and sea-ice brine from the High Arctic. *Fems Microbiology Ecology*. 2011;75(3):390-401.

8 Appendix A

8.1 MATERIALS AND METHODS

8.1.1 Analytical method OCPs and PBDEs

The lists of compounds included in the analytical method are shown in Table A.1 and A.2. Before extraction the samples are spiked with 25 ng each of a mix of ^{13}C -labelled compounds (POPs Pesticides HRMS Clean-up spike ^{13}C , Cambridge Isotope Laboratories). The individual surrogate standards are listed in Table A.1 and A.2. The samples are then Soxhlet extracted with 600 ml n-hexane/acetone (4:1, v/v) for eight hours at 75 °C. All the solvents used are glass-distilled grade from Rathburn (Walkerburn, UK). The solvent is evaporated with a rotary evaporator at 30 °C to about 5 ml. The extract is further evaporated to about 1 ml under a gentle stream of nitrogen at 20 °C. A 6 ml glass column packed with 1 g silica (Isolute®SPE, Biotage, Lund, Sweden) is conditioned with 5 ml n-hexane and the sample extract is passed through the column applying light vacuum. The analytes are eluted with 5 ml n-hexane followed by 5 ml n-hexane/dichloromethane (1:1, v/v). The two fractions are combined and evaporated under a gentle stream of nitrogen at 20 °C. The sample is reconstituted in 1 ml isooctane spiked with 25 ng $^{13}\text{C}_6$ -PCB-53 (Cambridge Isotope Laboratories) and analyzed by gas chromatography-high resolution mass spectrometry (GC-HRMS).

The gas chromatographic conditions for analysis of OCPs are the following: separation on a 60 m x 0.22 mm, 0.25 μm film thickness DB-5 MS column (Agilent Technologies, Santa Clara, CA, USA); carrier gas (He) at a flow of 0.8 ml min^{-1} ; splitless injection of 1 μl at 200 °C; temperature program 100 °C for 1 min, then 30 °C min^{-1} to 190 °C, and 2 °C min^{-1} to 290 °C, hold for 5 min. For the analysis of PBDEs the GC column used is a TR5 MS, 15 m x 0.25 mm x 0.1 μm (Thermo Scientific); the temperature program for PBDE analysis 120 °C for 2 min., 15 °C min^{-1} to 230 °C, 5 °C min^{-1} to 270 °C, 10 °C min^{-1} to 320 °C, hold for 5 minutes. The HRMS (DFS, Thermo Scientific, Bremen, Germany) is set up in the multiple ion detection modes (MID) at a resolution of 10,000 (10 % valley definition). Perfluorokerosene (PFK) is used as a reference compound to provide the inherent lock and calibration masses.

Table A.1. MS ions for Selected Ion Monitoring for OCPs and labeled recovery standard; detection limits for the compounds in atmospheric samples (given 5000 m³ as average sampling volume); average recoveries (%) of the labeled surrogate standards (\pm RSD%) and average field blanks.

Compound	Quantifier ion (m/z)	Qualifier ion (m/z)	MDL (pg m ⁻³)	Average field blanks (pg m ⁻³)
α -HCH	216.9145	218.9116	0.11	0.09
β -HCH	216.9145	218.9116	0.001	n.d.
γ -HCH	216.9145	218.9116	0.06	0.12
δ -HCH	216.9145	218.9116	0.04	0.004
Hexachlorobenzene	283.8102	285.8072	0.64	0.76
Heptachlor	271.8096	273.8067	0.007	0.001
Heptachlor epoxide	352.8442	354.8413	0.008	0.02
Aldrin	262.8564	264.8535	0.01	n.d.
Dieldrin	262.8564	264.8535	0.10	0.05
Endrin	262.8564	264.8535	0.10	n.d.
<i>trans</i> -Chlordane	372.8254	374.8225	0.03	0.004
<i>cis</i> -Chlordane	372.8254	374.8225	0.04	0.004
<i>trans</i> -Nonachlor	406.7864	408.7835	0.01	0.006
<i>cis</i> -Nonachlor	262.8564	264.8535	0.01	n.d.
Endosulfan I	338.8730	340.8700	0.004	0.02
Endosulfan II	262.8564	264.8535	0.006	n.d.
Endosulfan sulfate	262.8564	264.8535	0.04	0.06
<i>o,p'</i> -DDE	317.9345	318.9379	0.001	n.d.
<i>p,p'</i> -DDE	245.9998	247.9968	0.002	0.06
<i>o,p'</i> -DDD	235.0076	237.0046	0.01	n.d.
<i>p,p'</i> -DDD	235.0076	237.0046	0.008	0.001
<i>o,p'</i> -DDT	235.0076	237.0046	0.04	0.003
<i>p,p'</i> -DDT	235.0076	237.0046	0.003	0.01
Endrin ketone	247.8521	249.8921	0.003	n.d.
Methoxychlor	227.1067	228.1100	0.003	0.60

Surrogate standards			Recoveries %
α -HCH $^{13}\text{C}_6$	222.9341	224.9312	84 (\pm 25)
β -HCH $^{13}\text{C}_6$	222.9341	224.9312	63 (\pm 22)
γ -HCH $^{13}\text{C}_6$	222.9341	224.9312	102 (\pm 40)
δ -HCH $^{13}\text{C}_6$	222.9341	224.9312	136 (\pm 20)
Hexachlorobenzene $^{13}\text{C}_6$	289.8303	291.8273	82 (\pm 17)
Aldrin $^{13}\text{C}_{12}$	269.8799	271.8769	59 (\pm 10)
Dieldrin $^{13}\text{C}_{12}$	269.8799	271.8769	55 (\pm 18)
Endrin $^{13}\text{C}_{12}$	269.8799	271.8769	78 (\pm 16)
Heptachlor $^{13}\text{C}_{10}$	276.8264	278.8234	99 (\pm 13)
Heptachlor epoxide $^{13}\text{C}_{10}$	362.8772	364.8743	63 (\pm 9)
<i>trans</i> -Chlordane $^{13}\text{C}_{10}$	382.8590	384.8560	54 (\pm 19)
<i>trans</i> -Nonachlor $^{13}\text{C}_{10}$	416.8200	418.8170	59 (\pm 11)
<i>cis</i> -Nonachlor $^{13}\text{C}_{10}$	269.8799	271.8769	48 (\pm 20)
<i>o,p'</i> -DDE $^{13}\text{C}_{12}$	327.9777	329.9748	66 (\pm 16)
<i>p,p'</i> -DDE $^{13}\text{C}_{12}$	245.9998	247.9968	53 (\pm 11)
<i>o,p'</i> -DDD $^{13}\text{C}_{12}$	247.0481	249.0449	46 (\pm 16)
<i>p,p'</i> -DDD $^{13}\text{C}_{12}$	247.0481	249.0449	45 (\pm 20)
<i>o,p'</i> -DDT $^{13}\text{C}_{12}$	247.0481	249.0449	68 (\pm 15)
<i>p,p'</i> -DDT $^{13}\text{C}_{12}$	247.0481	249.0449	97 (\pm 27)
Recovery standard			
PCB-51 $^{13}\text{C}_6$	301.9626	303.9597	-

n.d. = not detected

Table A.2. MS ions for Selected Ion Monitoring for PBDEs and labeled surrogate standards; detection limits for the compounds in atmospheric samples (given 5000 m³ as average sampling volume); average recoveries (%) of the labeled surrogate standards (\pm RSD %) and average field blanks.

Compound	Quantifier ion (m/z)	Qualifier ion (m/z)	MDL ($\mu\text{g m}^{-3}$)	Average field blanks ($\mu\text{g m}^{-3}$)
BDE-17	405.8021	407.8001	0.01	0.001
BDE-28	405.8021	407.8001	0.02	0.009
BDE-47	485.7106	487.7085	0.12	0.06
BDE-66	485.7106	487.7085	0.02	0.004
BDE-71	485.7106	487.7085	0.01	0.009
BDE-85	563.6211	565.6190	0.03	0.001
BDE-99	563.6211	565.6190	0.07	0.04
BDE-100	563.6211	565.6190	0.03	0.009
BDE-138	481.6976	483.6956	0.04	0.002
BDE-153	481.6976	483.6956	0.03	0.01
BDE-154	481.6976	483.6956	0.03	0.009
BDE-183	561.6062	563.6042	0.04	0.06
BDE-190	561.6062	563.6042	0.06	0.002
Surrogate standards			Recoveries %	
BDE-28 ¹³ C ₁₂	417.8424	419.8403	106 (\pm 11)	
BDE-47 ¹³ C ₁₂	495.7529	497.7508	101 (\pm 11)	
BDE-99 ¹³ C ₁₂	575.6613	577.6593	99 (\pm 9)	
BDE-153 ¹³ C ₁₂	493.7372	495.7352	96 (\pm 16)	
BDE-154 ¹³ C ₁₂	493.7372	495.7352	90 (\pm 20)	
BDE-183 ¹³ C ₁₂	573.6457	575.6436	95 (\pm 10)	
Recovery standard				
PCB-51 ¹³ C ₆	301.9626	303.9597	-	

8.2 Analytical method neutral PFAS

The samples were spiked before extraction with 50 ng each of the following deuterium labeled compounds: 6:2, 8:2 and 10:2 FTOH D₅, MeFOSA D₃, EtFOSA D₅, MeFOSE D₇, and EtFOSE D₉ (Wellington Laboratories, Guelph, ON, Canada). Extraction was performed with a Soxhlet apparatus with MTBE/acetone (1/1, v/v) as solvent. After volume reduction isoctane was added as a

keeper and the extract was carefully evaporated under a stream of pure nitrogen, taking care that it would not evaporate to dryness. After reaching an approximate volume of 500 μl , the extract was transferred to a 1 ml volumetric flask and the volume was filled up with ethyl acetate containing $^{13}\text{C}_6$ -hexachlorobenzene as internal standard.

Analysis was done by an Agilent 5975C GC-MS (Agilent, Santa Clara, CA, USA) in selective ion monitoring mode (SIM) with positive chemical ionization (PCI) and methane as reagent gas. The analytes were separated on an Agilent CP-WAX 57 CB capillary column (25 m \times 0.25 mm \times 0.2 μm). The analyzed compounds and the details of the MS method are summarized in Table A.3.

Table A.3. MS ions for Selected Ion Monitoring for neutral PFAS and labeled surrogate standards; detection limits for the compounds in atmospheric samples (given 5000 m^3 as average sampling volume); average recoveries (%) of the labeled surrogate standards (\pm RSD %) and average field blanks.

Compound	Quantifier ion (m/z)	Qualifier ion (m/z)	MDL ($\mu\text{g m}^{-3}$)	Average field blanks ($\mu\text{g m}^{-3}$)
6:2 FTOH	365	327	0.45	0.04
8:2 FTOH	465	427	0.45	0.22
10:2 FTOH	565	527	0.20	0.11
N-Me-FOSA	514	-	0.20	0.10
N-Et-FOSA	528	-	0.22	0.13
N-Me-FOSE	540	558	0.15	0.19
N-Et-FOSE	554	572	0.11	0.15
Surrogate standards			Recoveries %	
6:2 FTOH D ₄	369	331	59 (\pm 22)	
8:2 FTOH D ₄	469	431	76 (\pm 24)	
10:2 FTOH D ₄	569	531	71 (\pm 35)	
N-Me-FOSA D ₃	517	-	87 (\pm 25)	
N-Et-FOSA D ₅	533	-	88 (\pm 22)	
N-Me-FOSE D ₇	547	565	119 (\pm 34)	
N-Et-FOSE D ₉	563	581	117 (\pm 33)	
Recovery standard				
Hexachlorobenzene $^{13}\text{C}_6$	291	293	-	

8.2.1 Analytical method HBCD

All filters were spiked with isomer-specific ^{13}C -labelled HBCD (Cambridge Isotope Laboratories (CIL), Tewksbury, MA, USA) and Soxhlet extracted with

hexane:acetone (4:1, v.v). The extracts were reduced in volume and cleaned on 2 g silica. After elution of other analytes with 100 ml hexane, the HBCD isomers were eluted with 20 ml hexane:dichloromethane (1:1, v:v). The eluates were dried under nitrogen, and the HBCD isomers were re-dissolved in 500 μ l methanol. The analysis was performed by high performance liquid chromatography (HPLC) with electrospray ionization in negative mode and tandem mass spectrometry detection (MS/MS).

The analysis included a procedural blank (pre-cleaned unexposed filter), which contained traces of the three isomers near detection limits, which all were subtracted from HBCD in the samples. Method detection limits (MDLs) were approximately 0.0047 pg m^{-3} for each isomer for the sample volume of 5000 m^3 . Filters spiked with 5.75 ng of each isomer gave recovery rates of 99.6 \pm 0.4, 101.5 \pm 0.5 and 98.5 % \pm 5.6 % for α -, β - and γ -HBCD, respectively.

9 Appendix B

9.1 List of publication connected to AMAP Core atmospheric part

Flyger H, Heidam NZ, Hansen KA, Rasmussen L, Megaw WJ. Background Levels of the Summer Tropospheric Aerosol and Trace Gases in Greenland. *Journal of Aerosol Science*. 1980;11(1):95-&.

Heidam NZ. Atmospheric Aerosol Factor Models, Mass and Missing Data. *Atmospheric Environment*. 1982;16(8):1923-31.

Heidam NZ. The Components of the Arctic Aerosol. *Atmospheric Environment*. 1984;18(2):329-43.

Davidson CI, Honrath RE, Kadane JB, Tsay RS, Mayewski PA, Lyons WB, et al. The Scavenging of Atmospheric Sulfate by Arctic Snow. *Atmospheric Environment*. 1987;21(4):871-82.

Davidson CI, Jaffrezo JL, Mosher BW, Dibb JE, Borys RD, Bodhaine BA, et al. Chemical-Constituents in the Air and Snow at Dye-3, Greenland .2. Analysis of Episodes in April 1989. *Atmospheric Environment Part A-General Topics*. 1993;27(17-18):2723-37.

Heidam NZ, Wåhlin P, Kemp K. Arctic Aerosols in Greenland. *Atmospheric Environment Part A-General Topics*. 1993;27(17-18):3029-36.

Christensen JH. The Danish Eulerian hemispheric model - A three-dimensional air pollution model used for the Arctic. *Atmospheric Environment*. 1997;31(24):4169-91.

Heidam NZ, Wåhlin P, Christensen JH. Tropospheric gases and aerosols in northeast Greenland. *Journal of the Atmospheric Sciences*. 1999;56(2):261-78.

Skov, H. Nielsdóttir, M.C. Goodsite, M.E. Christensen, J. Skjøth, C.A. Geernaert, G. Hertel, O. Olsen, J. (2003) "Measurements and modelling of gaseous elemental mercury on the Faroe Islands". *Asian Chemistry Letters* vol. 7, No. 2 & 3, 151-158.

Christensen, J.H. Brandt, J. Frohn, L.M. and Skov, H. (2004) "Modelling of mercury with the Danish Eulerian Hemispheric Model" *Atm. Chem. Phys.* vol. 4, 2251-2257.

Skov, H. Christensen, J. Goodsite, M.E. Heidam, N.Z. Jensen, B. Wåhlin, P. and Geernaert, G. (2004) "The fate of elemental mercury in Arctic during atmospheric mercury depletion episodes and the load of atmospheric mercury to Arctic" *ES & T.* vol. 38, 2373-2382.

Heidam, N.Z. Christensen, J.H. Skov, H. Wåhlin, P. (2004) Monitoring and modelling of the atmospheric Environment in Greenland. A review. *STOTEN.* vol. 331 No. 1-3, 5-28.

Goodsite, M.E. Plane, J.M. and Skov, H. (2004) A theoretical study of the oxidation of Hg⁰ to HgBr₂ in the troposphere. *ES&T.* vol 38, 1772-6.

- Ferrari, C.P. Dommergue A. Boutron, C.F. Skov, H. Goodsite, M. and Jensen, B. (2004) Night Production of Elemental Gaseous Mercury in Interstitial Air of Snow at Station Nord, Greenland shortly after Polar Sunrise. *Atm Env.* vol 38, 2727-2735.
- Hansen KM, Christensen JH, Brandt J, Frohn LM, Geels C. Modelling atmospheric transport of alpha-hexachlorocyclohexane in the Northern Hemisphere with a 3-D dynamical model: DEHM-POP. *Atmos Chem Phys.* 2004;4:1125-37.
- Bossi, R.; Vikelsøe, J.; Skov, H.; Petersen, D. (2005) Atmospheric concentrations of chlorinated pesticides, PCDD/Fs and c-PCBs in West Greenland: Organohalogen Compounds. vol. 67, s. 968-971.
- Fanou, L.A. Mobio, T.A. Creppy, E.E. Fayomi, B. Fustoni, S. Møller, P. Kyrtopoulos, S. Georgiades, P. Loft, S. Sanni, A. Skov H. Øvrebø S. and Autrup H. (2006) Survey of Air Pollution in Cotonou, benin-air monitoring and Biomarkers. *STOTEN.* vol 358. 85-96.
- Brooks, S. B., A. Saiz-Lopez, H. Skov, S. E Lindberg, J. M. C. Plane, and M. E. Goodsite (2006), The mass balance of mercury in the springtime arctic environment, *Geophys. Res. Lett.*, 33, L13812, doi:10.1029/2005GL025525.
- Skov, H. Wählin, P. Christensen, J. Heidam, N.Z. and Petersen, D. (2006) Measurements of elements, sulphate and SO₂ in Nuuk Greenland. *Atm. Env.* vol. 40, 4775-4781.
- Skov, H. Brooks, S. Goodsite, M.E. Lindberg, S.E. Meyers, T.P. Landis, M.S. Larsen, M.R.B. Jensen, B. McConville, G. Christensen, J. (2006) Measuring reactive gaseous mercury flux by relaxed eddy accumulation. *Atm. Env.* vol 40, 5452-5463.
- Hansen KM, Halsall CJ, Christensen JH. A dynamic model to study the exchange of gas-phase POPs between air and a seasonal snowpack. *Environ Sci Technol.* 2006;40(8):2644-52.
- Ariya, P.A. Skov, H. Grage M.L. and Goodsite M.E. (2008) Gaseous Elemental Mercury in the Ambient Atmosphere: Review of the Application of Theoretical Calculations and Experimental Studies for Determination of Reaction Coefficients and Mechanisms with Halogens and Other Reactants. *Advances in Quantum Chemistry* vol. 55, Chapter 4, 44-54.
- Bossi, R. Skov, H. Vorkamp, K. Christensen, J. Rastogi, S.C. Egeløv, A. and Petersen, D. (2008) Atmospheric concentrations of organochlorine pesticides, polybrominated diphenyl ethers and polychloronaphthalenes in Nuuk, South-West Greenland. *Atm. Env.* vol. 42, 7293-7303.
- Steffen, A. Douglas, T. Amyot, M. Ariya, P. Aspmo, K. Berg, T. Bottenheim, J. Brooks, S. Cobbett, F. Dastoor, A. Dommergue, A. Ebinghaus, R. Ferrari, C. Gårdfeldt, K. Goodsite, M. Lean, D. Poulain, A. Scherz, C. Skov, H. Sommar, J. and Temme, C. (2008) A synthesis of atmospheric mercury depletion event chemistry linking atmosphere, snow and water. *Atmospheric Chemistry and Physics.* vol. 8, 1445-1482.

- Johnson, M. S. Nilsson, E. J. K. Feilberg, K. L. Walter, S. Skov, H. Wallington, T. J. Röckmann, T. and Nielsen, C. J. Experimental studies of deuterium propagation through the atmospheric photochemical series CH₄, CH₃O, CH₂O, H₂. Geophysical Research Abstracts, Vol. 10, EGU2008-A-00000, 2008. EGU General Assembly 2008.
- Hansen KM, Halsall CJ, Christensen JH, Brandt J, Frohn LM, Geels C, et al. The role of the snowpack on the fate of alpha-HCH in an atmospheric chemistry-transport model. *Environ Sci Technol.* 2008;42(8):2943-8.
- Hung, H. Kallenborn, R. Breivik, K. Su, Y. Brorstrøm-Lunden, E. Olafsdottir, K. Leppanen, S. Bossi, R. Skov, H. Manø, S. Patton, G.W. Stern, G. Sverko, E. and Fellin P. (2010) Atmospheric Monitoring of Organic Pollutants in the Arctic under the Arctic Monitoring and Assessment Programme (AMAP): 1993-2006. *STOTEN.* vol. 408. 2854-2873. Doi: 10.1016/j.scitotenv.2009.10.044.
- Forsius M, Posch M, Aherne J, Reinds GJ, Christensen J, Hole L. Assessing the Impacts of Long-Range Sulfur and Nitrogen Deposition on Arctic and Sub-Arctic Ecosystems. *Ambio.* 2010;39(2):136-47.
- Møller, A.K. Barkay, T. Al-Soud, W.A, Sørensen, S.J. Skov, H. and Kroer, N. (2011) Diversity and characterization of mercury-resistant bacteria in snow, freshwater and sea-ice brine from the High Arctic; *FEMS Microbiol Ecol.* Vol. 75. 390-401.
- Hedegaard, G.B. Gross, A. Christensen, J.H. May, W. Skov, H. Geels, Hansen, K.M. and Brandt, J. (2011) Modelling the impact of climate change on tropospheric ozone over three centuries, *ACPD.* Vol. 11. 6805-6843. doi: 10.5194/acpd-11-6805-2011.
- Goodsite M. E.; Plane J. M. C.; Skov H. (2012). A Theoretical Study of the Oxidation of Hg⁰ to HgBr₂ in the Troposphere. Correction to *ES&T* vol 38, pg 1772, 2004) in *ES&T*, vol. 46, Issue: 9 5262-5262 DOI: 10.1021/es301201c.
- Douglas, T.A. Loseto, L. Macdonald, R. Outridge, P. Dommergue, A. Poulain, A. Amyot, M. Barkay, T. Berg, T. Chételat J. Constant, P. Evans, M. Ferrari, C. Gantner, N. Johnson, M. Kirk, J. Kroer, N. Larose, C. Lean, D. Muir, D. Nielsen, T.G. Poissant, L. Rognerud, S. Skov, H. Sørensen, S. Wang, F. Zdanowicz, C. M. (2012) The ultimate fate of mercury deposited to Arctic Marine and terrestrial ecosystems. *Env. Chem.* 9, 321-355.
- Fenger, M. Sørensen, L.L. Kristensen, K. Jensen B. Nøjgaard J.K. Massling, A. Skov, H. & Glasius, M. (2013) Sources of Anions in Aerosols in Northeast Greenland during Late Winter. *ACP*, vol. 13, 1-10 www.atmos-chem-phys-discuss.net/13/1/2013/doi:10.5194/acpd-13-1-2013.
- Nguyen, Q.T. Skov, H. Sørensen, L.-L. Jensen, B. Grube, A. G. Massling, A. Glasius, M. and Nøjgaard, J.K. (2013) Source apportionment of particulate matter at Station Nord, North East Greenland. *ACP.* Vol. 13, 35-49. www.atmos-chem-phys.net/13/35/2013/doi:10.5194/acp-13-35-2013.
- Bossi, R. Skjøth, C.A. and Skov, H. (2013) Three years (2008-2010) measurements of atmospheric concentrations of organochlorine pesticides (OCPs) at Station Nord, North East Greenland. *Environ. Sci.: Processes Impacts*, vol. 15 (12), 2213 - 2219. DOI: 10.1039/C3EM00304C.

Goodsite, M. Skov, H. Asmund, G. Bennike, O. Feilberg, A. Glasius, M. Gross, A. Hermanson, M.H. (2014) Pilot Study of Contaminants near Station Nord, a Military Airbase and Research Station in NE Greenland. NATO Advanced Research Workshop on Sustainable Cities and Military Installations: Climate Change Impact on Energy and Environmental Security. Conference paper 177-98. DOI: 10.1007/978-94-007-7161-1_10.

Hansen, A.M.K. Kristensen, K. Nguyen, Q.T. Zare, A. Cozzi, F. Nøjgaard, J.K. Skov, H. Brandt, J. Christensen, J.H. Ström, J. Tunved, P. Krejci, R. and Glasius, M. (2014) Organosulfates and organic acids in Arctic aerosols: Speciation, annual variation and concentration levels. ACP vol. 14, 1-17. doi: 10.5194/acpd-14-4745-2014.

Nguyen, Q. T., Kristensen, T. B. Hansen, A. M. K. Skov, H. Bossi, R. Massling, A. Sorensen, L. L. Bilde, M. Glasius, M. and Nøjgaard, J. K. (2014), Characterization of humic-like substances in Arctic aerosols, *Journal of Geophysical Research-Atmospheres*, 119(8), 5011-5027, doi:10.1002/2013jd020144.

Vorkamp, K. Bossi, R. Rigét, F.F. Skov, H. Sonne, C. and Dietz, R. (2015) Novel brominated flame retardants and dechlorane plus in Greenland air and biota. *Environmental Pollution* vol. 196. 284-291. <http://dx.doi.org/10.1016/j.envpol.2014.10.007>.

Massling, A., Nielsen, I. E., Kristensen, D., Christensen, J. H., Sørensen, L. L., Jensen, B., Nguyen, Q. T., Nøjgaard, J. K., Glasius, M., Skov, H., 2015, Atmospheric black carbon and sulfate concentrations in Northeast Greenland, *Atmospheric Chemistry and Physics*, Vol. 15, pp. 9681-9692, doi:10.5194/acp-15-9681-2015, available at: www.atmos-chem-phys.net/15/9681/2015/.

Eckhardt, S. Quennehen, B. Olivie, D. J. L. Berntsen, T. K. Cherian, R. Christensen, J. H. Collins, W. Crepinsek, S. Daskalakis, N. Flanner, M. Herber, A. Heyes, C. Hodnebrog, Ø. Huang, L. Kanakidou, M. Klimont, Z. Langner, J. Law, K. S. Lund, M. T. Mahmood, R. Massling, A. Myriokefalitakis, S. Nielsen, I. E. Nøjgaard, J. K. Quaas, J. Quinn, P. K. Raut, J.-C. Rumbold, S. T. Schulz, M. Sharma, S. Skeie, R. B. Skov, H. Uttal, T. von Salzen, K. and Stohl, A. (2015). Current model capabilities for simulating black carbon and sulfate concentrations in the Arctic atmosphere: a multi-model evaluation using a comprehensive measurement data set. *Atmos. Chem. Phys.* Vol. 15, 9413-9433. doi:10.5194/acp-15-9413-2015.

10 Appendix C

10.1 Abbreviations and wordlist

Table C.1. Wordlist for inorganic compounds

Ammonium	NH₄⁺
Black Carbon	Optically measured soot
Carbon dioxide	CO ₂
Carbon monoxide	CO
Chlorine	Cl
Gaseous elemental mercury	GEM
Mercury	Hg
Methane	CH ₄
Nitrate	NO ₃ ⁻
Ozone	O ₃
Sulphate	SO ₄ ²⁻
Sulphur Dioxide	SO ₂

Table C.2. Persistent organic compounds measured with a High Volume sampler sucking 500 L min⁻¹ through a filter and a PUF-XAD-PUF cartridge.

A. Chlorinated compounds:

Matrix	Acronym	Full name	Measured in biota
Air	HCB	Hexachlorobenzen	Yes
Air	α-HCH	α-hexachlorocyclohexane	Yes
Air	β-HCH	β-hexachlorocyclohexane	Yes
Air	γ-HCH (Lindane)	γ-hexachlorocyclohexane	Yes
Air	δ-HCH	δ-hexachlorocyclohexane	No
Air	Heptachlor	Heptachlor	No
Air	Heptachlor epoxide	Heptachlor epoxide	No
Air	Aldrin	Aldrin	No
Air	Dieldrin	Dieldrin	No
Air	Endrin	Endrin	No
Air	trans-Chlordane	trans-Chlordane	Yes
Air	cis-Chlordane	cis-Chlordane	Yes
Air	o,p'-DDT	o,p'-DDT	Yes
Air	p,p'-DDT	p,p'-DDT	Yes
Air	o,p'-DDE	o,p'-DDE	Yes
Air	p,p'-DDE	p,p'-DDE	Yes
Air	o,p'-DDD	o,p'-DDD	No
Air	p,p'-DDD	p,p'-DDD	Yes
Air	α-Endosulfan	α-Endosulfan	Yes*
Air	β-Endosulfan	β-Endosulfan	Yes*
Air	Endosulfan sulphate	Endosulfan sulphate	Yes*
Air	trans-Nonachlor	trans-Nonachlor	Yes
Air	cis-Nonachlor	cis-Nonachlor	Yes
Air	Endrin ketone	Endrin ketone	No
Air	Metoxychlor	Metoxychlor	No

*It is not part of the monitoring program but has been measured campaign wise (New Contaminant project).

Table C.2. Persistent organic compounds measured with a High Volume sampler sucking 500 L min⁻¹ through a filter and a PUF-XAD-PUF cartridge – continued:

B. Brominated compounds:

Matrix	Acronym	Full name	Measured in biota
Air	BDE 17	Polybrominated diphenylether 17	Yes
Air	BDE 28	Polybrominated diphenylether 28	Yes
Air	BDE 47	Polybrominated diphenylether 47	Yes
Air	BDE 66	Polybrominated diphenylether 66	Yes
Air	BDE 71	Polybrominated diphenylether 71	No
Air	BDE 85	Polybrominated diphenylether 85	Yes
Air	BDE 99	Polybrominated diphenylether 99	Yes
Air	BDE 100	Polybrominated diphenylether 100	Yes
Air	BDE 138	Polybrominated diphenylether 138	No
Air	BDE 153	Polybrominated diphenylether 153	Yes
Air	BDE 154	Polybrominated diphenylether 154	Yes
Air	BDE 183	Polybrominated diphenylether 183	Yes
Air	BDE 180	Polybrominated diphenylether 180	No
Air	BDE 209	Polybrominated diphenylether 209	Yes
Air	α-HBCD	α-Hexabromcyclododecane	Yes
Air	β-HBCD	β-Hexabromcyclododecane	Yes
Air	γ-HBCD	γ-Hexabromcyclododecane	Yes

*Other CAS-numbers for HBCD: 25637-99-4 or 3194-55-6; we do not have this number

C. Perfluoroalkyl substances (PFAS):

Matrix	Acronym	Full name	Measured in biota
Air	4:2 FTOH	4:2-fluorotelomer alcohol	No
Air	6:2 FTOH	6:2-fluorotelomer alcohol	No
Air	8:2 FTOH	8:2-fluorotelomer alcohol	No
Air	10:2 FTOH	10:2-fluorotelomer alcohol	No
Air	N-Me-FOSA	N-methyl-perfluorooctanesulfonamide	No
Air	N-Et-FOSA	N-ethyl-perfluorooctanesulfonamide	No
Air	N-Me-FOSE	N-methyl-perfluorooctanesulfonamidoethanol	No
Air	N-Et-FOSE	N-ethyl-perfluorooctanesulfonamidoethanol	No
Snow	PFBS	Perfluorobutane sulfonate	Yes
Snow	PFHxS	Perfluorohexane sulfonate	Yes
Snow	PFHpS	Perfluoroheptane sulfonate	Yes
Snow	PFOS	Perfluorooctane sulfonate	Yes
Snow	PFDS	Perfluorodecane sulfonate	Yes
Snow	PFOSA	Perfluorooctane sulfonamide	Yes
Snow	PFHxA	Perfluorohexanoic acid	Yes
Snow	PFHpA	Perfluoroheptanoic acid	Yes
Snow	PFOA	Perfluorooctanoic acid	Yes
Snow	PFNA	Perfluorononanoic acid	Yes
Snow	PFDA	Perfluorodecanoic acid	Yes
Snow	PFUnA	Perfluoroundecanoic acid	Yes
Snow	PFDoA	Perfluorododecanoic acid	Yes
Snow	PFTTrA	Perfluorotridecanoic acid	Yes
Snow	PFTeA	Perfluorotetradecanoic acid	Yes

Table C.3. Meteorological parameters measured at VRS.

Activities	Data availability	Instruments
Temperature	August 2014	
Relative humidity	August 2014	
Wind direction	August 2014	
Wind sped	August 2014	
Precipitation	August 2014	
Radiation blance	August 2014	
Snow depth	August 2014	
Boundary layer height	August 2014	Ceilometer
Vertical wind profile	Spring 2016	Wind LIDAR

Table C.4. List of elements analysed on filter packs sampled at VRS

Component	Fuld name
Al	Aluminium
As	Arsenic
Ba	Barium
Br	Bromine
Ca	Calcium
Cu	Copper
Cl	chlorine
Co	Cobalt
Cr	Chromium
Fe	Iron
Ga	Gallium
K	Potassium
Mg	Magnesium
Mn	Manganese
Mo	Molybdenum
Na	Sodium
Ni	Nickel
Pb	Lead
Rb	Rubidium
S	Sulphur
Sb	Antimony
Se	Selenium
Si	Silicon

AMAP CORE – ATMOSPHERIC PART
FROM 1990 TO 2015

ISBN: 978-87-7156-277-4
ISSN: 2245-019X